LBL-30963

Lawrence Berkeley Laboratory

UNIVERSITY OF CALIFORNIA

Physics Division

Mathematics Department

Numerical Study of Stokes Flows with Suspended Particles

E.Y. Tau
(Ph.D. Thesis)

July 1991

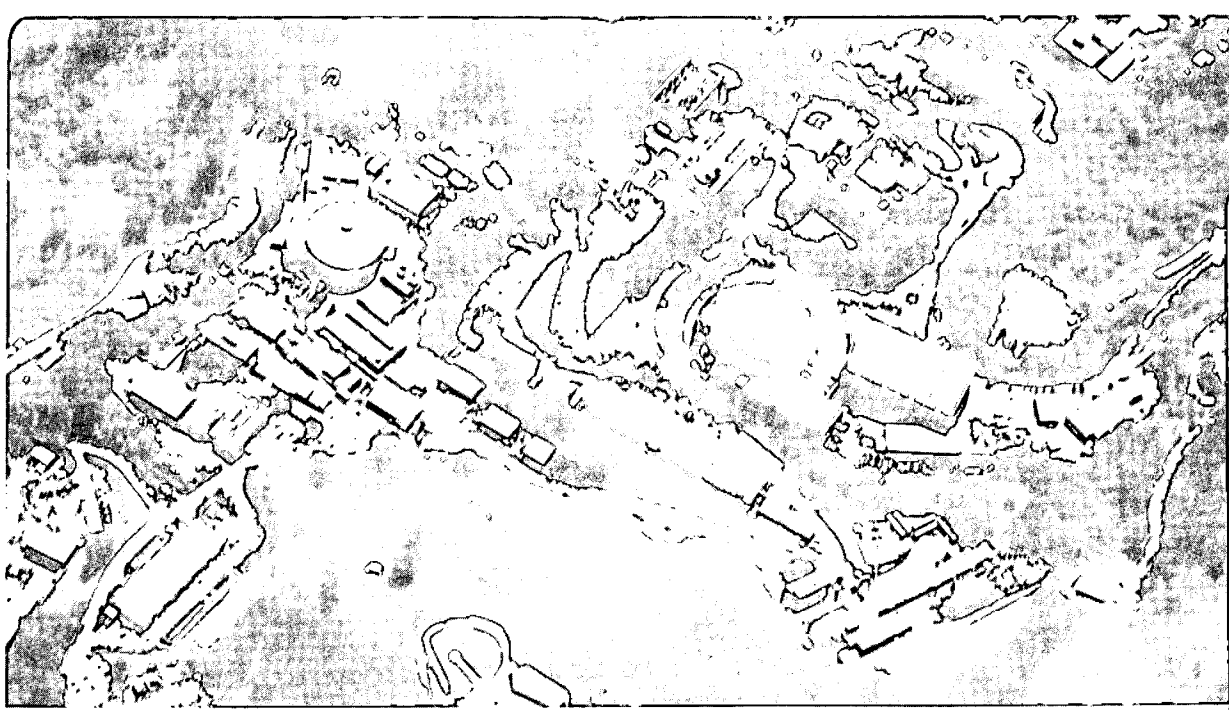

LOAN COPY
Circulates
for 4 weeks
Bldg. 50 Library.
LBL-30963
Copy 2

Prepared for the U.S. Department of Energy under Contract Number DE-AC03-76SF00098

DISCLAIMER

This document was prepared as an account of work sponsored by the United States Government. While this document is believed to contain correct information, neither the United States Government nor any agency thereof, nor the Regents of the University of California, nor any of their employees, makes any warranty, express or implied, or assumes any legal responsibility for the accuracy, completeness, or usefulness of any information, apparatus, product, or process disclosed, or represents that its use would not infringe privately owned rights. Reference herein to any specific commercial product, process, or service by its trade name, trademark, manufacturer, or otherwise, does not necessarily constitute or imply its endorsement, recommendation, or favoring by the United States Government or any agency thereof, or the Regents of the University of California. The views and opinions of authors expressed herein do not necessarily state or reflect those of the United States Government or any agency thereof or the Regents of the University of California.

LBL-30963

NUMERICAL STUDY OF STOKES FLOWS WITH SUSPENDED PARTICLES[1]

Eric Yu Tau

Ph.D. Thesis

Department of Mathematics
University of California
and
Lawrence Berkeley Laboratory
University of California
Berkeley, CA 94720

July 1991

[1] This work was supported by the Applied Mathematical Sciences subprogram of the Office of Energy Research, U.S. Department of Energy under Contract DE-AC03-76SF00098.

Numerical Study of Stokes Flows with Suspended Particles

by

Yu Tau

Abstract

We solve the Stokes equations in three space dimensions in the region outside a collection of spheres, with and without an outer boundary. The method of solution is the reflection method, in which one iteratively solves the problem outside each single sphere. The idea is to reduce the problem of finding a Stokes flow past a number of particles to a series of problems of finding a Stokes flow past one single particle. Our method can also be used to find the motion of sedimenting spheres.

We demonstrate numerically the convergence of the method for all sphere configurations in the case of unbounded domains. We use the method to find periodic solutions of the problem of three sedimenting spheres in a Stokes fluid. Long time periodic solutions are obtained when the initial positions of the spheres are symmetric and modulated long time scale periodic solutions are obtained when the initial positions are asymmetric.

We further develop a fast numerical algorithm for the solution of steady Stokes equations in a bounded domain in both two and three dimensions. The method is second order accurate and has an operation count of order $O(N \log N)$ where N is the number of grid points in the domain. We then use this algorithm to extend the method of reflections to bounded domains. The convergence of the method in this case is studied for various spheres configurations. The method is used to evaluate the effective viscosity of fluid with suspended spheres in a shear flow.

Contents

List of Figures iii

List of Tables iv

Introduction 1

Acknowledgements 4

1 Stokes Flow Outside a Single Sphere 5
- 1.1 Introduction 5
- 1.2 General Solutions 5
- 1.3 Force and Torque on the Sphere 10
- 1.4 Calculation of the Coefficients AX, BX etc. 12
- 1.5 Numerical Solutions and Examples 12

2 Interactions between Two or More Spheres 17
- 2.1 Introduction 17
- 2.2 The Method of Reflections 18
- 2.3 Force and Torque on a Sphere 20
- 2.4 Some Numerical Examples 20
- 2.5 Method of Reflections Applied to Sedimentation 22

3 Numerical Solution of the Steady Stokes Equations 27
- 3.1 Introduction 27
- 3.2 Discretization of the Domain and Choice of D^h, ∇^h, Δ_h 31
- 3.3 Solution of the Equations 34
- 3.4 Other Boundary Conditions 38

4 Stokes Flows in Bounded Domains and Evaluation of Effective Viscosity 41
- 4.1 Introduction 41
- 4.2 Numerical examples 43
- 4.3 Application to the Evaluation of Effective Viscosity 44

5 Discussion and Conclusion 47

Bibliography 50

Figures 54

List of Figures

2.1 Velocity field of the two sphere problem 54
2.2 Convergence of the method of reflections 54
2.3 Velocity field of the 4 sphere configuration 55
2.4 Velocity field of the 9 sphere configuration 56
2.5 Three spheres falling down under gravity 57
2.6 Symmetric initial position 58
2.7 Symmetric initial position, result 1 59
2.8 Symmetric initial position, result 2 59
2.9 Asymmetric initial position 60
2.10 Asymmetric initial position, result 1 61
2.11 Asymmetric initial position, result 2 61
2.12 Asymmetric initial position, result 3 62
2.13 Asymmetric initial position, result 4 62
3.1 Discretization of Domain 63
3.2 Velocity field of steady Stokes flow in 2-D 63
4.1 Velocity field of one sphere in a box 64
4.2 Velocity field of two spheres in a box 64
4.3 Velocity field of three spheres in a box 65
4.4 Velocity field of five spheres in a box 65
4.5 Velocity field of seven spheres in a box 66
4.6 Shear flow suspension with one sphere 67
4.7 Effective viscosity of shear flow suspension with one sphere 67
4.8 Shear flow suspension with two sphere 68
4.9 Effective viscosity of shear flow suspension with two spheres 68

List of Tables

1.1 Accuracy of the approximation for different N 16
1.2 Accuracy of the approximation for different M 16
1.3 Accuracy of the approximation for different d 16

2.1 Resistance coefficients of two equal spheres 21
2.2 Convergent rate for different number of spheres 21
2.3 End velocity of three falling spheres 25
2.4 Half period of sedimentation of three spheres, time step $\delta t = 0.1$ 26

3.1 Numerical results in 2-D case 36
3.2 Numerical results in 3-D case 37
3.3 Iterations needed for a different discretization 38
3.4 Numerical results in 3-D case for periodic conditions 39

4.1 Convergent rate for a sphere fixed in a box 43
4.2 Convergent rate for two spheres fixed in a box 44

Introduction

Low Reynolds number flow of fluids with suspended particles has been of great interest to both engineers and scientists for a long time. Its applications can be found in a very broad range of problems from polymer dynamics in chemical engineering to blood flow in biology. Because of the complicated boundary conditions required to satisfy the no-slip condition on the surfaces of particles, it is generally not possible to obtain exact solutions of these problems, so some approximations have to be used.

One of the first and simplest is the point force approximation ([7]- [8], [29], [39], [6], [5], and[38]). In this method each particle is replaced by a point force and the no slip condition on the particles surface is satisfied only in some average sense. Since point forces radiate with equal intensity in all directions the angular dependence of the disturbances on one particle's surface produced by the other particles cannot be taken into account. Recently the collocation method was developed ([16], [17] and [21]) in which the solution to Stokes equations is expanded in the appropriate eigenfunctions and the boundary conditions are satisfied at some collocation points. Brady, Bossis and coworkers also developed a very cost-efficient technique they called the Stokesian dynamics ([3], [13], [4]). A brief review and comparison of the two methods can be found in the paper by Weinbaum, Ganatos and Yan ([41]). Other methods include boundary integral method ([42], [17] and [40]).

In this thesis we present a numerical study of Stokes flow with suspended particles by the method of reflections. The method of reflections presented here was introduced by Smoluchowsi ([31]) in 1911 and has been used to study the Stokes flow with suspended particles by many people (see, e.g. [31], [32], [9], [25], [19] and [22]). This method is a iterative method. It depends on the linearity of the Stokes equations and reduces the problem to a series solutions of Stokes flows outside a single particle. There exists no rigorous proof that the method converges. In a recent paper by Luke [27], it is proven that

in a bounded domain the method converges in the energy dissipation norm, assume that the flow ooutside a single particle in a bounded region is known. However the solution of Stokes equations outside a single particle in a bounded domain is itself far from trivial and in addition the proof breaks down for an unbounded domain. We use numerical computations to study the convergence of the method of reflections in an unbounded domain and extend the method to a bounded domain by treating the boundary of the domain in a manner analygous to the treatment of the particles. In all our computations we assume the particles are spheres.

In chapter 1, the solution of Stokes equations outside a single sphere in an unbounded domain is obtained using the method of harmonic expansions, for any given velocity condition on the surface of the sphere. The expansion is then truncated for numerical computation. A Gaussian quadrature formula is used in the numerical integration of the coefficients of the expansion. The accuracy of the solution is studied via comparison with some simple known exact solutions.

In chapter 2 we present the method of reflections based on the solution outside a single sphere we obtained in chapter 1. We study numerically the convergence of the method for flows pass a number of fixed spheres. We test the method on closely packed sphere configurations. In all these cases our numerical computations show the method is convergent. This has convinced us that the method is convergent in unbounded domains. Next we modify the method to solve problems in which the forces and torques on the spheres are given and apply the method to find the periodic solutions of the problem of three sedimenting spheres. Long time periodic solutions are obtained when the initial positions of the spheres are symmetric, and the results agree well with previous work done by Caflisch *et al.* [10]. Modulated periodic solutions on a long time scale are also obtained when the initial positions are asymmetric. All these calculations demonstrate the convergence of the method.

In chapter 3 a fast numerical technique for finding solutions of the steady-state Stokes equations without particles in both two and three dimensional domains is presented. We implement the method on a special staggered grid for a rectangular (cubic) domain, and obtain a solution in an order of $O(N \log N)$ operations for both two and three dimensional cases, where N is the number of grid points in the domain. The main idea is to derive from the Stokes equations an equation for the pressure p, $Ap = b$, where the matrix A is semi-positive definite and very well conditioned on the orthogonal complement of its null

space.

In chapter 4 we combine the methods described in chapter 2 and 3 to extend the method of reflections to a bounded domain. The convergence of the method in this case is studied for different sphere configurations. We then apply the method to the evaluation of effective viscosity of particle suspension in a shear flow. Our numerical results show good agreement with Einstein's formula [14] when the particle volume fraction is small.

Finally chapter 5 contains the discusssion and conclusions suggested by our numerical results. The silarity and difference of our method and the collocation technique of Ganatos *et al.* [15] will also be discussed.

Acknowledgements

I would like to thank my thesis advisor, Alexandre Chorin, for his encouragement and advice. It has been a pleasure and a privilege to be his student.

I would like to thank Ole Hald for his careful reading of the draft, and Philip Marcus for serving as the outside reader.

I would also like the thank late Mr. K. C. Wong and K. C. Wong Educational Foundation for providing me the loan which made it possible for me to come to the United State to pursue my Ph.D degree.

I am grateful to my wife Bo Yu, for her love and support during the five years of my graduate study.

Chapter 1

Stokes Flow Outside a Single Sphere

1.1 Introduction

In this chapter we develop a numerical solution of Stokes equations outside a single sphere in an unbounded domain. The solution will form the basis for the method of reflections in chapter 2 for treating Stokes flow with more than one sphere.

1.2 General Solutions

We want to solve the following problem:

$$\mu \nabla^2 \vec{u} = \nabla p, \tag{1.1}$$

$$\nabla \cdot \vec{u} = 0. \tag{1.2}$$

with boundary conditions on the surface of the sphere given by

$$\vec{u}_{(r=a,\theta,\phi)} = \vec{V}_{(\theta,\phi)} \tag{1.3}$$

and

$$\vec{u}_{(r=\infty,\theta,\phi)} = 0. \tag{1.4}$$

Using spherical coordinates, the general solution of Eq. (1) and (2) is given by Lamb [26] and by Happel and Brenner [19],

$$\vec{u} = \sum_{n=-\infty}^{+\infty} \left[\nabla \times (\vec{r}\chi_n) + \nabla\Phi_n + \frac{n+3}{2\mu(n+1)(2n+3)} r^2 \nabla p_n - \frac{n}{\mu(n+1)(2n+3)} \vec{r} p_n, \right] \tag{1.5}$$

where χ_n, Φ_n and p_n are solid spherical harmonics, and $p = \sum_{n=-\infty}^{+\infty} p_n$ is the pressure.

Since we require $\vec{u}\,|_{r=\infty} = 0$, we must have

$$p_n = \Phi_n = \chi_n = 0 \qquad \text{for} \quad n \geq 1$$

so that

$$\vec{u} = \sum_{n=1}^{\infty} \left[\nabla \times (\vec{r}\chi_{-(n+1)}) + \nabla\Phi_{-(n+1)} - \frac{n-2}{2\mu n(2n-1)} r^2 \nabla p_{-(n+1)} + \frac{n+1}{\mu n(2n-1)} \vec{r} p_{-(n+1)} \right]. \tag{1.6}$$

Now we describe a general method for obtaining harmonic functions $p_{-(n+1)}$, $\Phi_{-(n+1)}$ and $\chi_{-(n+1)}$ that satisfy the boundary condition (1.3), we follow the outline given by Happel and Brenner [19].

For the radial component of velocity, since it is always true that

$$(\nabla \times (\vec{r}\chi_n))_r = 0$$

for any χ_n, we find

$$u_r = \sum_{n=1}^{\infty} \left[\frac{\partial \Phi_{-(n+1)}}{\partial r} - \frac{n-2}{2\mu n(2n-1)} r^2 \frac{\partial p_{-(n+1)}}{\partial r} + \frac{n+1}{\mu n(2n-1)} r p_{-(n+1)} \right]. \tag{1.7}$$

By virtue of Euler's theorem for homogeneous polynomials,

$$r\frac{\partial h_n}{\partial r} = n h_n, \tag{1.8}$$

where h_n is any solid spherical harmonics of order n, we may simplify Eq. (1.7) to,

$$u_r = \sum_{n=1}^{\infty} \left[\frac{n+1}{2\mu(2n-1)} r p_{-(n+1)} - \frac{n+1}{r} \Phi_{-(n+1)} \right]. \tag{1.9}$$

Differentiation of Eq. (1.9) with respect to r and again applying Euler's theorem gives

$$r\frac{\partial \vec{u}_r}{\partial r} = \sum_{n=1}^{\infty}\left[\frac{n(n+1)}{2\mu(2n-1)}rp_{-(n+1)} + \frac{(n+1)(n+2)}{r}\Phi_{-(n+1)}\right]. \tag{1.10}$$

In addition to these relationships we can also obtain, by taking the curl of Eq. (1.6) and dot product with vector $\vec{r}$,

$$\vec{r}\cdot\nabla\times\vec{u} = \sum_{n=1}^{\infty} n(n+1)\chi_{-(n+1)}. \tag{1.11}$$

Thus, at the surface of the sphere we obtain

$$[u_r]_a = \sum_{n=1}^{\infty}\left(\frac{na}{2\mu(2n-1)}[p_{-(n+1)}]_a - \frac{n+1}{a}[\Phi_{-(n+1)}]_a\right), \tag{1.12}$$

$$\left[r\frac{\partial u_r}{\partial r}\right]_a = \sum_{n=1}^{\infty}\left(\frac{n(n+1)a}{2\mu(2n-1)}[p_{-(n+1)}]_a + \frac{(n+1)(n+2)}{a}[\Phi_{-(n+1)}]_a\right), \tag{1.13}$$

$$[\vec{r}\cdot\nabla\times\vec{u}]_a = \sum_{n=1}^{\infty} n(n+1)[\chi_{-(n+1)}]_a, \tag{1.14}$$

where the subscript a denotes evaluation of the function at $r = a$.

If $\vec{V} = \vec{V}(\theta,\phi)$ denotes the value of the velocity field on the sphere surface, that is,

$$\vec{V} = [\vec{u}]_a$$

then it may be shown that

$$[u_r]_a = \frac{\vec{r}}{r}\cdot\vec{V}, \tag{1.15}$$

$$\left[r\frac{\partial u_r}{\partial r}\right]_a = -r\nabla\cdot\vec{V}, \tag{1.16}$$

$$[\vec{r}\cdot\nabla\times\vec{u}]_a = \vec{r}\cdot\nabla\times\vec{V}, \tag{1.17}$$

where ∇ is the usual three-dimensional nabla operator. The second of these relationships depends upon the validity of the continuity equation $\nabla\cdot\vec{u} = 0$ whereas the remaining two equations are true for an arbitrary vector function $\vec{u}$. Because of the properties of solid spherical harmonics, we have

$$[p_n]_a = \left(\frac{a}{r}\right)^n p_n \tag{1.18}$$

with two similar identities for χ_n and Φ_n. Introduction of these relations into Eqs. (1.12) - (1.14) gives us

$$\begin{aligned}\frac{\vec{r}}{r}\cdot\vec{V} &= \sum_{n=1}^{\infty}\left[\frac{na}{2\mu(2n-1)}\left(\frac{a}{r}\right)^{-(n+1)} p_{-(n+1)}\right.\\ &\quad\left.-\frac{n+1}{a}\left(\frac{a}{r}\right)^{-(n+1)}\Phi_{-(n+1)}\right],\end{aligned} \tag{1.19}$$

$$\begin{aligned}-r\nabla\cdot\vec{V} &= \sum_{n=1}^{\infty}\left[\frac{n(n+1)a}{2\mu(2n-1)}\left(\frac{a}{r}\right)^{-(n+1)} p_{-(n+1)}\right.\\ &\quad\left.+\frac{(n+1)(n+2)}{a}\left(\frac{a}{r}\right)^{-(n+1)}\Phi_{-(n+1)}\right],\end{aligned} \tag{1.20}$$

$$\vec{r}\cdot\nabla\times\vec{V} = \sum_{n=1}^{\infty}\left[n(n+1)\left(\frac{a}{r}\right)^{-(n+1)}\chi_{-(n+1)}\right]. \tag{1.21}$$

Since $\frac{\vec{r}}{r}\cdot\vec{V}, -r\nabla\cdot\vec{V}$ and $\vec{r}\cdot\nabla\times\vec{V}$ are all functions of (θ,ϕ) only, we can expand them in terms of surface spherical harmonics as

$$\frac{\vec{r}}{r}\cdot\vec{V} = \sum_{n=1}^{\infty} X_n,$$

$$-r\nabla\cdot\vec{V} = \sum_{n=1}^{\infty} Y_n,$$

$$\vec{r}\cdot\nabla\times\vec{V} = \sum_{n=1}^{\infty} Z_n.$$

Thus we have

$$\begin{aligned}\sum_{n=1}^{\infty} X_n &= \sum_{n=1}^{\infty}\left[\frac{na}{2\mu(2n-1)}\left(\frac{a}{r}\right)^{-(n+1)} p_{-(n+1)}\right.\\ &\quad\left.-\frac{n+1}{a}\left(\frac{a}{r}\right)^{-(n+1)}\Phi_{-(n+1)}\right],\end{aligned} \tag{1.22}$$

$$\begin{aligned}\sum_{n=1}^{\infty} Y_n &= \sum_{n=1}^{\infty}\left[\frac{n(n+1)a}{2\mu(2n-1)}\left(\frac{a}{r}\right)^{-(n+1)} p_{-(n+1)}\right.\\ &\quad\left.+\frac{(n+1)(n+2)}{a}\left(\frac{a}{r}\right)^{-(n+1)}\Phi_{-(n+1)}\right],\end{aligned} \tag{1.23}$$

$$\sum_{n=1}^{\infty} Z_n = \sum_{n=1}^{\infty} \left[n(n+1) \left(\frac{a}{r}\right)^{-(n+1)} \chi_{-(n+1)} \right]. \tag{1.24}$$

Equating term-by-term under the summation sign, and solving the three resultant equations for the harmonic functions $p_{-(n+1)}, \Phi_{-(n+1)}$ and $\chi_{-(n+1)}$, we obtain

$$p_{-(n+1)} = \frac{\mu(2n-1)}{n+1} \frac{1}{a} \left(\frac{a}{r}\right)^{n+1} [(n+2)X_n + Y_n], \tag{1.25}$$

$$\Phi_{-(n+1)} = \frac{1}{2(n+1)} a \left(\frac{a}{r}\right)^{n+1} (nX_n + Y_n), \tag{1.26}$$

$$\chi_{-(n+1)} = \frac{1}{n(n+1)} \left(\frac{a}{r}\right)^{n+1} Z_n. \tag{1.27}$$

In our computation each X_n, Y_n and Z_n are expressed in terms of the associated Legendre functions and the sin, cos functions as

$$X_n(Y_n, Z_n) = \sum_{m=0}^{n} P_n^m(\cos\theta)(A_n^m \cos m\phi + B_n^m \sin m\phi).$$

If we express $\vec{V}$ in the spherical coordinates as

$$\vec{V} = (V_r, V_\theta, V_\phi)$$

and keep in mind that $\vec{V}$ is a function of θ and ϕ only, we find

$$\frac{\vec{r}}{r} \cdot \vec{V} = V_r(\theta, \phi), \tag{1.28}$$

$$-r\nabla \cdot \vec{V} = -\left[2V_r + \frac{1}{\sin\theta} \frac{\partial}{\partial\theta} (\sin\theta\, V_\theta) + \frac{1}{\sin\theta} \frac{\partial V_\phi}{\partial\phi} \right] \tag{1.29}$$

and

$$\vec{r} \cdot \nabla \times \vec{V} = \frac{1}{\sin\theta} \frac{\partial}{\partial\theta} (\sin\theta\, V_\phi) - \frac{1}{\sin\theta} \frac{\partial V_\theta}{\partial\phi}. \tag{1.30}$$

Now we expand each term in those equations in terms of associated Legendre functions and sin, cos functions to obtain

$$V_r = \sum_{n=1}^{\infty} \sum_{m=0}^{n} P_n^m(\cos\theta)(AX_n^m \cos m\phi + BX_n^m \sin m\phi),$$

$$\frac{1}{\sin\theta} \frac{\partial}{\partial\theta} (\sin\theta\, V_\theta) = \sum_{n=1}^{\infty} \sum_{m=0}^{n} P_n^m(\cos\theta)(AY1_n^m \cos m\phi + BY1_n^m \sin m\phi),$$

$$\frac{1}{\sin\theta}\frac{\partial V_\phi}{\partial\phi} = \sum_{n=1}^{\infty}\sum_{m=0}^{n} P_n^m(\cos\theta)(AY2_n^m\cos m\phi + BY2_n^m\sin m\phi),$$

$$\frac{1}{\sin\theta}\frac{\partial}{\partial\theta}(\sin\theta\, V_\phi) = \sum_{n=1}^{\infty}\sum_{m=0}^{n} P_n^m(\cos\theta)(AZ1_n^m\cos m\phi + BZ1_n^m\sin m\phi),$$

$$\frac{1}{\sin\theta}\frac{\partial V_\theta}{\partial\phi} = \sum_{n=1}^{\infty}\sum_{m=0}^{n} P_n^m(\cos\theta)(AZ2_n^m\cos m\phi + BZ2_n^m\sin m\phi).$$

Finally, we have the expressions for X_n, Y_n and Z_n as

$$X_n = \sum_{m=0}^{n} P_n^m(\cos\theta)(AX_n^m\cos m\phi + BX_n^m\sin m\phi), \tag{1.31}$$

$$Y_n = \sum_{m=0}^{n} P_n^m(\cos\theta)(AY_n^m\cos m\phi + BY_n^m\sin m\phi), \tag{1.32}$$

$$Z_n = \sum_{m=0}^{n} P_n^m(\cos\theta)(AZ_n^m\cos m\phi + BZ_n^m\sin m\phi), \tag{1.33}$$

where

$$AY_n^m = -\left(2AX_n^m + AY1_n^m + AY2_n^m\right), \tag{1.34}$$

$$BY_n^m = -\left(2BX_n^m + BY1_n^m + BY2_n^m\right), \tag{1.35}$$

$$AZ_n^m = AZ1_n^m - AZ2_n^m, \tag{1.36}$$

$$BZ_n^m = BZ1_n^m - BZ2_n^m. \tag{1.37}$$

1.3 Force and Torque on the Sphere

Once the velocity field has been found, the force and torque (about the sphere center) exerted on the sphere by the fluid can be calculated. Let Π be the stress tensor, then

$$\vec{F} = \int_S \vec{\Pi}_r dS,$$

$$\vec{T}_O = \int_S \vec{r}\times\vec{\Pi}_r dS.$$

It can be shown that (see, e.g., [26] and [19])

$$\vec{\Pi}_r = \frac{\vec{r}}{r}\cdot\Pi = -\frac{\vec{r}}{r}p + \mu\left(\frac{\partial\vec{u}}{\partial r} - \frac{\vec{u}}{r}\right) + \frac{\mu}{r}\nabla(\vec{r}\cdot\vec{u}).$$

Using Eq. (1.6), we obtain the formula

$$\vec{\Pi}_r = \frac{\mu}{r}\sum_{n=1}^{\infty}\Big[-(n+2)\nabla\times(\vec{r}\chi_{-(n+1)}) - 2(n+2)\nabla\Phi_{-(n+1)} + \frac{n^2-1}{2\mu n(2n-1)}r^2\nabla p_{-(n+1)} - \frac{2n^2+1}{2\mu n(2n-1)}\vec{r}p_{-(n+1)}\Big]. \tag{1.38}$$

Substitution of Eq. (1.38) into the surface integrals for $\vec{F}$ and $\vec{T}_O$, with the help of following identities for arbitrary solid spherical harmonic functions H

$$\int_S H_{-(n+1)}dS = 0 \quad \text{for all } n \geq 1,$$

$$\int_S \vec{r}H_{-(n+1)}dS = \begin{cases} \frac{4\pi r}{3}\nabla(r^3H_{-2}) & \text{for } n = 1 \\ 0 & \text{for all other } n \end{cases}$$

$$\int_S \nabla H_{-(n+1)}dS = 0 \quad \text{for all } n \geq 1,$$

and

$$\int_S \nabla\times(\vec{r}H_{-(n+1)})dS = 0 \quad \text{for all } n,$$

eventually gives us

$$\vec{F} = -4\pi\nabla(r^3p_{-2}) \tag{1.39}$$

$$\vec{T}_O = -8\pi\mu\nabla(r^3\chi_{-2}) \tag{1.40}$$

or, in term of coefficients AX_n^m etc. , we have

$$F_x = -2\mu a(3AX_1^1 + AY_1^1),$$

$$F_y = -2\mu a(3BX_1^1 + BY_1^1),$$

$$F_z = -2\mu a(3AX_1^0 + AY_1^0)$$

and

$$T_O^x = -4\mu a^2 AZ_1^1,$$

$$T_O^y = -4\mu a^2 BZ_1^1,$$

$$T_O^z = -4\mu a^2 AZ_1^0.$$

1.4 Calculation of the Coefficients AX, BX etc.

Now we proceed to describe the numerical calculations of all the coefficients. It is well known (see, e.g., [23]) that we can express the coefficients as

$$\begin{bmatrix} AX_n^m \\ BX_n^m \end{bmatrix} = c_n^m \int_0^{2\pi}\int_0^{\pi} V_r P_n^m(\cos\theta) \begin{bmatrix} \cos m\phi \\ \sin m\phi \end{bmatrix} \sin\theta d\theta d\phi, \tag{1.41}$$

$$\begin{aligned} \begin{bmatrix} AY1_n^m \\ BY1_n^m \end{bmatrix} &= c_n^m \int_0^{2\pi}\int_0^{\pi} \frac{1}{\sin\theta}\frac{\partial}{\partial\theta}(\sin\theta\, V_\theta)\, P_n^m(\cos\theta) \begin{bmatrix} \cos m\phi \\ \sin m\phi \end{bmatrix} \sin\theta d\theta d\phi \\ &= -c_n^m \int_0^{2\pi}\int_0^{\pi} V_\theta \frac{dP_n^m}{d\theta} \begin{bmatrix} \cos m\phi \\ \sin m\phi \end{bmatrix} \sin\theta d\theta d\phi, \end{aligned} \tag{1.42}$$

$$\begin{aligned} \begin{bmatrix} AY2_n^m \\ BY2_n^m \end{bmatrix} &= c_n^m \int_0^{2\pi}\int_0^{\pi} \frac{1}{\sin\theta}\frac{\partial V_\phi}{\partial\phi} P_n^m(\cos\theta) \begin{bmatrix} \cos m\phi \\ \sin m\phi \end{bmatrix} \sin\theta d\theta d\phi \\ &= m c_n^m \int_0^{2\pi}\int_0^{\pi} V_\phi P_n^m \begin{bmatrix} \sin m\phi \\ -\cos m\phi \end{bmatrix} d\theta d\phi, \end{aligned} \tag{1.43}$$

$$\begin{aligned} \begin{bmatrix} AZ1_n^m \\ BZ1_n^m \end{bmatrix} &= c_n^m \int_0^{2\pi}\int_0^{\pi} \frac{1}{\sin\theta}\frac{\partial}{\partial\theta}(\sin\theta\, V_\phi)\, P_n^m(\cos\theta) \begin{bmatrix} \cos m\phi \\ \sin m\phi \end{bmatrix} \sin\theta d\theta d\phi \\ &= -c_n^m \int_0^{2\pi}\int_0^{\pi} V_\phi \frac{dP_n^m}{d\theta} \begin{bmatrix} \cos m\phi \\ \sin m\phi \end{bmatrix} \sin\theta d\theta d\phi, \end{aligned} \tag{1.44}$$

$$\begin{aligned} \begin{bmatrix} AZ2_n^m \\ BZ2_n^m \end{bmatrix} &= c_n^m \int_0^{2\pi}\int_0^{\pi} \frac{1}{\sin\theta}\frac{\partial V_\theta}{\partial\phi} P_n^m(\cos\theta) \begin{bmatrix} \cos m\phi \\ \sin m\phi \end{bmatrix} \sin\theta d\theta d\phi \\ &= m c_n^m \int_0^{2\pi}\int_0^{\pi} V_\theta P_n^m \begin{bmatrix} \sin m\phi \\ -\cos m\phi \end{bmatrix} d\theta d\phi, \end{aligned} \tag{1.45}$$

where

$$c_n^m = \frac{(2n+1)(n-m)!}{2\pi\delta_m(n+m)!} \qquad \delta_m = \begin{cases} 2 & m = 0 \\ 1 & m \neq 0 \end{cases}$$

The surface integral is calculated numerically by using Gaussian quadrature formulas [36]. We divide the surface integrals in Eqs. (1.41) - (1.45) into two categories, those

that have the form

$$I_1 = \int_0^{2\pi}\int_0^{\pi} f(\theta,\phi)\sin\theta d\theta d\phi$$

and those have the form

$$I_2 = \int_0^{2\pi}\int_0^{\pi} f(\theta,\phi) d\theta d\phi.$$

Each can be approximated by Gaussian quadrature formula as

$$I_1 = \sum_{i=1}^{M}\sum_{j=1}^{2M} f(\theta_i^1,\phi_j)C_i^1 D_j^1 \tag{1.46}$$

and

$$I_2 = \sum_{i=1}^{M}\sum_{j=1}^{2M} f(\theta_i^2,\phi_j)C_i^2 D_j^2, \tag{1.47}$$

where

$$\theta_i^1 = \cos^{-1}(x_i),$$

$$\phi_j = \pi + \pi y_j,$$

$$\theta_i^2 = 0.5\pi(1 + x_i),$$

in which x_i, y_j are roots of appropriate Legendre polynomials, and the C_i^1, D_j^1, C_i^2, D_j^2 are the corresponding quadrature weights (see e.g. [36]).

1.5 Numerical Solutions and Examples

To evaluate the velocity numerically, the infinite series of the right hand side of Eq. (1.6) has to be truncated after finite number of terms, say N. Thus we obtain

$$\begin{aligned}\vec{u} \;=\; \sum_{n=1}^{N}\Big[&\nabla\times(\vec{r}\chi_{-(n+1)}) + \nabla\Phi_{-(n+1)} - \frac{n-2}{2\mu n(2n-1)}r^2\nabla p_{-(n+1)} \\ &+\frac{n+1}{\mu n(2n-1)}\vec{r}p_{-(n+1)}\Big].\end{aligned} \tag{1.48}$$

For computational purpose, we substitute Eqs. (1.25) - (1.27) and Eqs. (1.31) - (1.33) into Eq. (1.48) to obtain

$$\begin{aligned}u \;=\; \sum_{n=1}^{N}\sum_{m=0}^{2n}\Big[&a^{i+1}A_n^m\left(z\frac{\partial}{\partial y}YY_n^m - y\frac{\partial}{\partial z}YY_n^m\right) + a^{i+2}B_n^m\frac{\partial}{\partial x}YY_n^m \\ &+ a^i C_n^m\left(s_n^1 xYY_n^m - s_n^2 r^2\frac{\partial}{\partial x}YY_n^m\right)\Big],\end{aligned} \tag{1.49}$$

$$v = \sum_{n=1}^{N}\sum_{m=0}^{2n}\left[a^{i+1}A_n^m\left(x\frac{\partial}{\partial z}YY_n^m - z\frac{\partial}{\partial x}YY_n^m\right) + a^{i+2}B_n^m\frac{\partial}{\partial y}YY_n^m + a^iC_n^m\left(s_n^1 yYY_n^m - s_n^2 r^2\frac{\partial}{\partial y}YY_n^m\right)\right], \tag{1.50}$$

$$w = \sum_{n=1}^{N}\sum_{m=0}^{2n}\left[a^{i+1}A_n^m\left(y\frac{\partial}{\partial x}YY_n^m - x\frac{\partial}{\partial y}YY_n^m\right) + a^{i+2}B_n^m\frac{\partial}{\partial x}YY_n^m + a^iC_n^m\left(s_n^1 zYY_n^m - s_n^2 r^2\frac{\partial}{\partial z}YY_n^m\right)\right] \tag{1.51}$$

where

$$x = r\sin\theta\cos\phi$$

$$y = r\sin\theta\sin\phi$$

$$z = r\cos\theta$$

are Cartesian coordinates,

$$s_n^1 = \frac{n+1}{n(2n-1)}$$

$$s_n^2 = \frac{n-2}{2n(2n-1)}$$

and for $m = 0,\ldots,n$

$$A_n^m = \frac{1}{n(n+1)}AZ_n^m$$

$$B_n^m = \frac{1}{2(n+1)}\left(nAX_n^m + AY_n^m\right)$$

$$C_n^m = \frac{(2n-1)}{n+1}\left((n+2)AX_n^m + AY_n^m\right)$$

$$YY_n^m = \frac{1}{r^{n+1}}P_n^m(\cos\theta)\cos m\phi$$

for $m = n+1,\ldots,2n$

$$A_n^m = \frac{1}{n(n+1)}BZ_n^{m-n}$$

$$B_n^m = \frac{1}{2(n+1)}\left(nBX_n^{m-n} + BY_n^{m-n}\right)$$

$$C_n^m = \frac{(2n-1)}{n+1}\left((n+2)BX_n^{m-n} + BY_n^{m-n}\right)$$

$$YY_n^m = \frac{1}{r^{n+1}}P_n^{m-n}(\cos\theta)\sin(m-n)\phi.$$

As a numerical example, we take $a = 1$ and

$$\vec{u} = \Omega\vec{e}_y - (\alpha + \beta z + \gamma z^2)\vec{e}_x \quad on \quad r = 1.$$

In this case the exact solution is known to be (see [22])

$$\vec{u} = (u, v, w),$$

$$\begin{aligned} u &= -\frac{A}{2}\left(1+\frac{x^2}{r^2}\right)\frac{1}{r} - B\left(1-\frac{3x^2}{r^2}\right) - C\frac{z}{r^3} \\ &+\frac{3D}{2}\left(\frac{zx^2}{r^5}\right) + 3E\left(1-\frac{5x^2}{r^2}\right)\frac{z}{r^5} + 3F\left(\frac{z^2-y^2}{r^2}\right)\frac{1}{r^3} \\ &-\frac{G}{10}\left(1-\frac{13x^2+5z^2}{r^2}+\frac{75z^2x^2}{r^4}\right)\frac{1}{r^3} \\ &+3H\left(1-\frac{5x^2+5z^2}{r^2}+\frac{35z^2x^2}{r^4}\right)\frac{1}{r^5}, \end{aligned} \tag{1.52}$$

$$\begin{aligned} v &= -\frac{A}{2}\left(\frac{xy}{r^3}\right) + 3B\left(\frac{xy}{r^5}\right) + \frac{3D}{2}\left(\frac{xyz}{r^5}\right) - 15E\frac{xyz}{r^7} + 3F\frac{xy}{r^5} \\ &+\frac{G}{10}\left(13-\frac{75z^2}{r^2}\right)\frac{xy}{r^5} - 15H\left(1-\frac{7z^2}{r^2}\right)\frac{xy}{r^7}, \end{aligned} \tag{1.53}$$

$$\begin{aligned} w &= -\frac{A}{2}\left(\frac{zx}{r^3}\right) + 3B\left(\frac{zx}{r^5}\right) + C\frac{x}{r} + \frac{3D}{2}\left(\frac{z^2x}{r^5}\right) - 3E\left(1-\frac{5z^2}{r^2}\right)\frac{x}{r^5} \\ &-3F\frac{zx}{r^5} + \frac{G}{10}\left(23-\frac{75z^2}{r^2}\right)\frac{xz}{r^5} - 15H\left(3-\frac{7z^2}{r^2}\right)\frac{zx}{r^7}, \end{aligned} \tag{1.54}$$

where

$$A = \frac{3}{2}\left(\alpha - \frac{1}{3}\gamma\right),\ B = \frac{1}{4}\left(\alpha - \frac{3}{5}\gamma\right),\ C = -\left(\Omega - \frac{1}{2}\beta\right),$$
$$D = -\frac{3}{5}\beta,\ E = -\frac{1}{6}\beta,\ F = -\frac{1}{9}\gamma,\ G = \frac{7}{12}\gamma,\ H = \frac{1}{24}\gamma.$$

To see how good the approximation (1.48) is and how the accuracy varies with different choice of parameters, we make a number of numerical computations. For our first calculation, we want to check how the accuracy of approximation (1.48) changes with the increase of N while the number of points used in the Gaussian quadrature formulas is fixed, i.e., M is fixed. Table 1.1 shows the result of this calculation. The error is measured by the maximum absolute value of the difference between the exact solution and the numerical

Table 1.1: Accuracy of the approximation for different N

N	1	2	3	4
$e(u)$	0.4469	0.1414	7.919×10^{-3}	8.557×10^{-3}
$e(v)$	0.1907	7.275×10^{-2}	3.861×10^{-3}	5.536×10^{-3}
$e(w)$	0.4080	0.1716	5.425×10^{-3}	5.388×10^{-3}

Table 1.2: Accuracy of the approximation for different M

M	2	3	4	5	7
$e(u)$	0.7671	0.1708	2.548×10^{-2}	7.919×10^{-3}	2.114×10^{-4}
$e(v)$	0.8514	0.1035	1.935×10^{-2}	3.861×10^{-3}	1.238×10^{-4}
$e(w)$	0.6594	0.1753	1.939×10^{-2}	5.425×10^{-3}	1.126×10^{-4}

solution on the surface of a certain distance away from the center of the sphere. We chose $M = 5$, the distance $d = 1.5a = 1.5$ and $\Omega = \alpha = \beta = \gamma = 1$.

From the results, we see that the accuracy increase rapidly with N except for $N = 4$. The reason for this is that the exact solution of this particular problem only contains terms up to $N = 3$.

Next we look at how the accuracy changes with the increase of M. Table 1.2 displays the results of this computation with $N = 3$ and other parameters remain the same. We can obtain reasonable approximation with $M = 4$.

Finally table 1.3 shows how the approximation varies with the distance away from the center of the sphere. The parameters are chosen as $N = 3$, $M = 5$, and others remain unchanged. The conclusion is that our approximation is very accurate when d becomes large compared to the radius a.

Table 1.3: Accuracy of the approximation for different d

d	1	1.2	1.5	2	5
$e(u)$	4.847×10^{-2}	2.113×10^{-2}	7.919×10^{-3}	3.341×10^{-3}	2.894×10^{-4}
$e(v)$	1.383×10^{-2}	5.857×10^{-3}	3.861×10^{-3}	1.950×10^{-3}	1.336×10^{-4}
$e(w)$	1.297×10^{-2}	6.454×10^{-3}	5.425×10^{-3}	2.985×10^{-3}	2.184×10^{-4}

Chapter 2

Interactions between Two or More Spheres

2.1 Introduction

In this chapter we shall consider the interactions between a number of rigid spheres moving slowly in an unbounded viscous fluid. We assume the motion outside the spheres is governed by the quasi-static Stokes equations, and the velocity, $\vec{U}_i$, angular velocity, $\vec{\Omega}_i$, and the position, $\vec{x}_i$, $i = 1, \ldots, N$, of each sphere are given. Then we have the following equations,

$$\mu \nabla^2 \vec{u} = \nabla p, \tag{2.1}$$

$$\nabla \cdot \vec{u} = 0, \tag{2.2}$$

and boundary conditions

$$\vec{u}_i = \vec{U}_i + (\vec{x} - \vec{x}_i) \times \vec{\Omega}_i \quad \vec{x} \in \partial B_i, \quad i = 1, \ldots, n. \tag{2.3}$$

Because of the complicated boundary conditions, it is in general not possible to find the exact solution of Eq. (2.1) - (2.3). The only exact solutions known so far are those for the slow motion of two spheres (see, for instance, [34] and [18]). Therefore much effort has been made to find good approximate solutions. Some of the approximations being long used are point-force approximation ([7], [8], [29], [39], [6] , [5] and [38]) and the method of reflections ([31], [32], [9], [25] and [19]). More recently, the collocation technique was

developed ([16], [17], [15], and [21]). In the point-force approximation, each sphere is replaced by a point force and the no slip condition on the sphere surface is satisfied only in some average sense. Since point forces radiate with equal intensity in all directions the angular dependence of the disturbances on the sphere surface by the others cannot be taken into account. The collocation technique requires that the no slip condition be satisfied at some discrete points on the surface, but the method generally requires some symmetry of the flow under consideration, and the selection of the points at which the no slip condition is to be satisfied could be very subtle. The method of reflections is an iterative method. It satisfies the no slip condition on each sphere surface one by one. The rate of convergence of this method depend strongly on the ratio of sphere spacing to the sphere diameter. When the ratio is close to one, the convergence can be very slow.

2.2 The Method of Reflections

Assume we have n spheres $B_i, i = 1, \ldots, n$, at the positions $\vec{x}_i$, with given velocities $\vec{U}_i$ and angular velocities $\vec{\Omega}_i$. We want to find a Stokes flow that satisfies the no slip boundary condition on the surface of each sphere. We have

$$\left.\begin{array}{l} \mu\nabla^2\vec{u} = \nabla p, \\ \nabla\cdot\vec{u} = 0. \end{array}\right\} \quad \vec{x} \in \mathbf{R}^n - B, \quad B = \bigcup B_i$$

$$\vec{u}_i = \vec{U}_i + (\vec{x} - \vec{x}_i) \times \vec{\Omega}_i \quad \vec{x} \in \partial B_i, \quad i = 1, \ldots, n. \tag{2.4}$$

Since the equations and boundary conditions are linear, we can write the solution as

$$\vec{u} = \vec{u}^{(1)} + \vec{u}^{(2)} + \vec{u}^{(3)} + \ldots \tag{2.5}$$

with each term separately satisfies the equations of motion and vanishes at infinity. Again, because of linearity, each term $\vec{u}^{(i)}$ can be divided into sum of a finite terms as

$$\vec{u}^{(i)} = \vec{u}_1^{(i)} + \ldots + \vec{u}_n^{(i)} \tag{2.6}$$

The method of reflections is to successively satisfy the no slip boundary conditions on the surface of each sphere. We proceed as follows: first pick one of n spheres, say B_1, use the method we described in Chapter 1 to find $\vec{u}_1^{(1)}$ such that

$$\vec{u}_1^{(1)} = \vec{U}_1 + (\vec{x} - \vec{x}_1) \times \vec{\Omega}_1 \quad on \quad \partial B_1, \tag{2.7}$$

then find $\vec{u}_2^{(1)}$ so that

$$\vec{u}_2^{(1)} = \vec{U}_2 + (\vec{x} - \vec{x}_2) \times \vec{\Omega}_2 - \vec{u}_1^{(1)} \quad on \quad \partial B_2, \tag{2.8}$$

$$\cdots \quad \cdots \quad \cdots$$

and $\vec{u}_n^{(1)}$ such that

$$\vec{u}_n^{(1)} = \vec{U}_n + (\vec{x} - \vec{x}_n) \times \vec{\Omega}_n - \sum_{j=1}^{n-1} \vec{u}_j^{(1)} \quad on \quad \partial B_n. \tag{2.9}$$

This completes one step of reflection. Step two starts with finding $\vec{u}_1^{(2)}$ such that

$$\vec{u}_1^{(2)} = \vec{U}_1 + (\vec{x} - \vec{x}_1) \times \vec{\Omega}_1 - \vec{u}^{(1)} \quad on \quad \partial B_1, \tag{2.10}$$

So at step k for sphere i, we find $\vec{u}_i^{(k)}$ such that

$$\vec{u}_i^{(k)} = \vec{U}_i + (\vec{x} - \vec{x}_i) \times \vec{\Omega}_i - \sum_{j=1}^{k-1} \vec{u}^{(j)} - \sum_{l=1}^{i-1} \vec{u}_l^{(k)} \quad on \quad \partial B_i. \tag{2.11}$$

This procedure is continued until the no slip conditions on the surfaces of all the spheres are satisfied to the approximation desired. For later references, we call the velocity field $\vec{u}_i^{(k)}$ the reflection of sphere i at step k. As pointed out in [19], there exists no rigorous proof that this procedure converges to the right solution. In a recent paper [27], it has been proven that for a bounded domain the method converges in the energy dissipation norm. In the proof each velocity field $\vec{u}_i^{(k)}$ always satisfies the given velocity condition on the boundary of the domain. The proof breaks down for an unbounded domain. However, a heuristic convergence argument can be given as follows: assume we have n spheres of radius a, and characteristic distance between them d, and assume at step k the boundary conditions on the surface of each sphere are satisfied within order U. To satisfy the condition on sphere number one will generate a velocity field of order $U\frac{a}{d}$ on the surfaces of the other spheres, which is less than U. When we try to satisfy the no slip condition for other spheres, we will generate a velocity field which is of order $U\frac{a}{d}$ on the surface of sphere one. Thus the no slip condition of sphere one is satisfied within an order of $U\frac{a}{d}$, that is we gain an order of accuracy of the boundary condition.

2.3 Force and Torque on a Sphere

Once the velocity field is computed to the degree of approximation desired, the force $\vec{F}_i$ and torque $\vec{T}_i$ exerted on each sphere by the fluid is obtained by summing the contributions of the individual fields. Since a closed surface integral of a function with no singularities in the interior of the surface is always zero, a velocity field which has no singularities in the interior of a sphere can produce neither a resultant force nor torque on the sphere. Thus contribution to the force and torque on a sphere is made only by those velocity fields generated to satisfy the boundary conditions on its own surface, hence

$$\vec{F}_i = \vec{F}_i^{(1)} + \vec{F}_i^{(2)} + \vec{F}_i^{(3)} + \dots \tag{2.12}$$

$$\vec{T}_i = \vec{T}_i^{(1)} + \vec{T}_i^{(2)} + \vec{T}_i^{(3)} + \dots \tag{2.13}$$

where $\vec{F}_i^{(j)}$ and $\vec{T}_i^{(j)}$ are force and torque generated by velocity field $\vec{u}_i^{(k)}$, respectively. Using the notation in chapter 1, we find

$$F_{i,x} = -2\mu a \sum_k (3AX_{1,i}^{1,k} + AY_{1,i}^{1,k}) = -2\mu a \sum_k C_{1,i}^{1,k}, \tag{2.14}$$

$$F_{i,y} = -2\mu a \sum_k (3BX_{1,i}^{1,k} + BY_{1,i}^{1,k}) = -2\mu a \sum_k C_{1,i}^{2,k}, \tag{2.15}$$

$$F_{i,z} = -2\mu a \sum_k (3AX_{1,i}^{0,k} + AY_{1,i}^{0,k}) = -2\mu a \sum_k C_{1,i}^{0,k} \tag{2.16}$$

and

$$T_{i,x} = -4\mu a^2 \sum_k AZ_{1,i}^{1,k} = -4\mu a^2 \sum_k A_{1,i}^{1,k}, \tag{2.17}$$

$$T_{i,y} = -4\mu a^2 \sum_k BZ_{1,i}^{1,k} = -4\mu a^2 \sum_k A_{1,i}^{2,k}, \tag{2.18}$$

$$T_{i,z} = -4\mu a^2 \sum_k AZ_{1,i}^{0,k} = -4\mu a^2 \sum_k A_{1,i}^{0,k}. \tag{2.19}$$

2.4 Some Numerical Examples

Now we apply the method just developed to some simple problems. The quantities we calculate are the coefficients A_n^m, B_n^m and C_n^m in Eqs. (49) - (51) in chapter 1 for each velocity field $\vec{u}_k^{(i)}$ in Eqs. (2.5) and (2.6). When all the coefficients A_n^m, B_n^m and C_n^m for the latest velocity field $\vec{u}^{(i)}$ are smaller in absolute value than some predefined tolerance ϵ, then the computation stops and we say that the method converged in i steps. Once the

Table 2.1: Resistance coefficients of two equal spheres

M	k	f1	f2	(f1+f2)/2	exact
5	29	0.65025779	0.63964662	0.6449522	
7	32	0.64704579	0.64294489	0.6449953	0.64500
9	32	0.64501947	0.64497012	0.6449948	

Table 2.2: Convergent rate for different number of spheres

ns	2	4	10	30	50	100	150
k	29	38	37	37	38	37	36

ns: number of spheres, k: number of steps, $\epsilon = 5 \times 10^{-5}$

coefficients are computed, we can easily obtain the final velocity field using Eqs. (49) - (51) in chapter 1 and Eqs. (2.5) and (2.6), and the force and torque on each sphere using Eqs. (2.14) - (2.19).

First we look at a two sphere problem where the two spheres are fixed in an otherwise uniform flow along the line of centers (see Fig. 2.1). In this special case the exact solution to the problem can be obtained using bipolar coordinates system (see [34]). In table 2.1 we compare the resistance coefficient for each sphere obtained using our numerical method with those of the exact solution in the case where the two spheres are at their closest position (which is the worst situation for our method). The resistance coefficient is defined as the ratio of the force exerted on the sphere by the fluid to the force when there is only one sphere, namely

$$f = \frac{F}{6\pi\mu a U}$$

where a is the radius of the spheres and U is the speed of the uniform flow. In our computation we have chosen N in Eq. (48) in chapter 1 to be 3 and $\epsilon = 5 \times 10^{-5}, k$ in table 2.1 is the number of steps needed for the method to converge. As we can see the results of our method are very accurate when the integrals in the evaluation of coefficients are calculated accurately.

Next we look at the convergence of the method. In table 2.2 we list the number of steps it takes for the method to converge for different numbers of spheres all lined up along a line through their centers (see Fig. 2.2).

We can see that when the number of spheres is greater than 4, the number of steps

does not change very much. From that we can conclude that the rate of convergence of the method is only determined by the spacing of a very small number of neighboring spheres.

In the next few examples, we consider some of the most closely packed sphere configurations for this problem. In all our computations we use a tolerance $\epsilon = 1 \times 10^{-5}$. In figure 2.3 we have 4 spheres fixed in a otherwise uniform flow. The method achieves convergence in 30 steps. We also achieve convergence for a 8 sphere configuration with two layers of 4 spheres as in figure 2.3, one on top of the other, in 37 steps. In figure 2.4 we have a total of 27 spheres with 3 layers of 9 sphere configuration. Again the method converges in just 45 steps. In our last example we look at the problem where 13 spheres packed together with one in the middle such that the centers of other 12 spheres form a regular dodecahedron. In is shown in a recent paper by W. Hsiang [24] that this configuration will achieve the optimal upper bound of local density for sphere packing. We obtain the convergence for the method of reflections for this case in 262 steps. Those computational results suggest that the method of reflections is convergent for all sphere configurations in an unbounded domain.

2.5 Method of Reflections Applied to Sedimentation

So far we only used the method of reflections to solve problems when the motion of spheres is given. It is also possible to use the method to solve problems where the force and torque on each sphere are given instead. Assume we are given force F_i^∞ and torque T_i^∞ on each sphere. To simplify our notation, we define

$$\mathbf{F} = \{F_1, F_2, \ldots, F_n, T_1, \ldots, T_n\},$$

$$\mathbf{U} = \{U_1, U_2, \ldots, U_n, \Omega_1, \ldots, \Omega_n\},$$

$$m = \{m_1, m_2, \ldots, m_n\}$$

and

$$J = \{J_1, J_2, \ldots, J_n\}$$

where n is the number of spheres in consideration, and U_i, Ω_i, m_i and J_i are the velocity, angular velocity, mass and inertial moment fo each sphere, respectively.

It is shown in [19] that

$$\mathbf{F} = \mathbf{R}\mathbf{U}$$

where the resistance matrix $\mathbf{R}$ is independent of $\mathbf{U}$. $\mathbf{R}$ is also symmetric, as can be shown from the reciprocal theorem, and positive definite, due to the dissipative nature of the system [13] .

If we let the spheres move in the following way,

$$\mathbf{m}\frac{d\mathbf{U}}{dt} = -\mathbf{F}^{\infty} + \mathbf{R}\mathbf{U} \tag{2.20}$$

$$\mathbf{U}_{(t=0)} = \mathbf{U}^0$$

where $\mathbf{m} = \{m, J\}$, then since $\mathbf{R}$ is positive definite, and if $\mathbf{F}^{\infty} = \mathbf{R}\mathbf{U}^{\infty}$ for some $\mathbf{U}^{\infty}$, we have

$$\lim_{(t\to\infty)} \mathbf{U} = \mathbf{U}^{\infty}$$

for any initial $\mathbf{U}^0$.

To solve this problem using the method of reflections, we solve Eq. (2.20) numerically by the Euler's method,

$$\mathbf{U}^{(k+1)} = \left(-\mathbf{F} + \mathbf{R}\mathbf{U}^k\right)\delta t + \mathbf{U}^k. \tag{2.21}$$

Start with the initial condition $\mathbf{U}^0 = 0$. The matrix $\mathbf{R}$ is calculated using the method of reflections implicitly, i.e. given a $\mathbf{U}$ we Use the method to find an $\mathbf{F} = \mathbf{R}\mathbf{U}$.

For computational purposes, we need to scale Eq. (2.21) so that our choice of δt can be independent of radii of the spheres. To do that, we decompose the matrix $\mathbf{R}$ in the following block form

$$\mathbf{R} = \begin{pmatrix} \mathbf{R}_{FV} & \mathbf{R}_{F\Omega} \\ \mathbf{R}_{TV} & \mathbf{R}_{T\Omega} \end{pmatrix}$$

and

$$\mathbf{U} = (\mathbf{V}, \mathbf{\Omega})^t,$$

then Eq. (2.20) becomes

$$m\frac{d\mathbf{V}}{dt} = -F^{\infty} + \mu\left(\mathbf{R}_{FV}\mathbf{V} + \mathbf{R}_{F\Omega}\mathbf{\Omega}\right), \tag{2.22}$$

$$J\frac{d\mathbf{\Omega}}{dt} = -T^{\infty} + \mu\left(\mathbf{R}_{TV}\mathbf{V} + \mathbf{R}_{T\Omega}\mathbf{\Omega}\right). \tag{2.23}$$

Now let $[M], [L]$ and $[t]$ be the units of mass, length and time, respectively, Then the units of other quantities are, if we let each variable with a square bracket represents its corresponding unit,

$$[V] = \frac{[L]}{[t]}, \quad \Omega = \frac{1}{[t]}, \quad [\mu] = \frac{[M]}{[t][L]},$$
$$[F] = \frac{[M][L]}{[t]^2}, \quad [T] = \frac{[M][L]^2}{[t]^2}.$$

By dimensional analysis, we find

$$[F] = [\mu][\mathbf{R}_{FV}][V]$$

so

$$\frac{[M][L]}{[t]^2} = \frac{[M]}{[t][L]}[\mathbf{R}_{FV}]\frac{[L]}{[t]},$$

which gives

$$[\mathbf{R}_{FV}] = [L].$$

If we consider a as the characteristic radius of the spheres, we obtain

$$\mathbf{R}_{FV} = O(a).$$

Similarly, we can obtain

$$\mathbf{R}_{R\Omega} = O(a^2), \quad \mathbf{R}_{TV} = O(a^2), \quad \mathbf{R}_{T\Omega} = O(a^3).$$

We define the following nondimensional variables,

$$F' = \frac{F}{mg}, \quad T' = \frac{T}{\mu U_0 a^2}, \quad U' = \frac{U}{U_0}, \quad \Omega' = \frac{\Omega a}{U_0}, \quad t' = \frac{ta\mu}{m}$$

and

$$\mathbf{R}'_{FV} = \frac{\mathbf{R}_{FV}}{a}, \quad \mathbf{R}'_{F\Omega} = \frac{\mathbf{R}_{F\Omega}}{a^2}, \quad \mathbf{R}'_{TV} = \frac{\mathbf{R}_{TV}}{a^2}, \quad \mathbf{R}'_{T\Omega} = \frac{\mathbf{R}_{T\Omega}}{a^3}$$

where $U_0 = \dfrac{mg}{6\mu\pi a}$. Using the relation $J = \dfrac{2}{5}ma^2$ Eqs. (2.22) and (2.23) become

$$\frac{dV'}{dt'} = -6\pi F' + \mathbf{R}'_{FV}V' + \mathbf{R}'_{F\Omega}\Omega'$$
$$\frac{d\Omega'}{dt'} = \frac{5}{2}\left(-T + \mathbf{R}'_{TV}V' + \mathbf{R}'_{T\Omega}\Omega'\right).$$

As a simple example, we look at the problem where we have three equal sized spheres falling down under gravity in a same vertical plane. We want to find the velocities

and angular velocities of the spheres when the steady state is achieved. We assume at the steady state three spheres lie on the vertices of a right angled triangle (see fig. 2.5) at points (0,0,0), (-1,0,0) and (0,1,0). The direction of gravity is taken as the x axis. The parameters are chosen as

$$a = 0.1, \quad \mu = 1, \quad \delta t' = 0.1$$

The results are shown in table 2.3.

Table 2.3: End velocity of three falling spheres

sphere	1	2	3
u_x	0.320554	0.287839	0.320161
u_y	-0.000101	0.011333	0.013526
u_z	0.0	0.0	0.0
w_x	0.0	0.0	0.0
w_y	0.0	0.0	0.0
w_z	-0.038818	0.056213	-0.014889

Next we consider the sedimentation of three equal spheres which are originally located in a same horizontal plane. It is proven in [10] that if enough symmetry is imposed initially, the relative motion of the three spheres is periodic in time. We would like to reproduce the solution by using the method of reflections. In this sedimentation problem, the spheres are assumed to move according to the velocity generated by the gravity and the forces induced by other spheres, i.e.

$$\frac{d\mathbf{x}_i}{dt} = \mathbf{V}_i(\mathbf{x}) \tag{2.24}$$

where $\mathbf{V}_i$ (and $\mathbf{\Omega}_i$) is such that the force (and torque) on each sphere is zero.

We use the following scheme to solve Eq. (2.24):

$$\mathbf{x}_i^{(n+\frac{1}{2})} = \mathbf{x}_i^n + \mathbf{V}_i(\mathbf{x}^n)\delta t \tag{2.25}$$

$$\mathbf{x}_i^{(n+1)} = \mathbf{x}_i^n + \frac{1}{2}\left(\mathbf{V}_i(\mathbf{x}^n) + \mathbf{V}_i(\mathbf{x}^{(n+\frac{1}{2})})\right)\delta t \tag{2.26}$$

We first present the results for symmetric configurations. We calculate the relative positions of the spheres $y = x_2 - x_1, z = x_3 - x_1$. Initially the sphere centers are located at points $x_1 = (0,0,0), x_2 = (0,1,1), x_3 = (0,1,-1)$ (see fig. 2.6). The results of our computation are shown in figure 2.7 and 2.8 and table 2.4.

Table 2.4: Half period of sedimentation of three spheres, time step $\delta t = 0.1$

a	0.1	0.2	0.3	0.5	0.6	0.65
T/2	6.5	6.6	6.7	8.1	9.4	10.3

We can see that our results are in good agreement with those in [10] except for $a = 0.65$. Now we look at the asymmetric initial configuration where the sphere are centered at $(0,0,0),(0,0.5,1),(0,1.5,-1)$ (see fig. 2.9).

A nearly periodic solution is obtained for a short time scale, as in good agreement with the results in [10] (see fig. 2.10). If we keep our computation for a long time, a modulated periodic solution in a long time scale begins to appear, as is displayed in figure 2.11 - 2.13. This result suggests that for the sedimentation of three spheres, the relative motion will be always periodic as long as they stay close together.

Chapter 3

Numerical Solution of the Steady Stokes Equations

3.1 Introduction

In this chapter, we describe a fast numerical technique for finding solutions of the steady-state Stokes equations in both two and three dimensional domains. When we combine this technique with the method of reflections for an unbounded domain described in chapter 2, we will have in chapter 4 a method for finding Stokes flows in bounded domains in chapter 4.

For simplicity, we describe the problem in the two dimensional case. The Stokes equations have the following form:

$$-\mu\Delta\mathbf{u} + \nabla p = \mathbf{f} \tag{3.1}$$

$$\nabla \cdot \mathbf{u} = 0 \tag{3.2}$$

where $\mathbf{u} = (u, v)$ is the velocity field, p is the pressure, $\mathbf{f} = (f_x, f_y)$ is the body force and μ is the viscosity of the fluid. Let Ω be a rectangular domain. We assume the following boundary condition on $\mathbf{u}$:

$$\mathbf{u}(x, y) = \mathbf{u}_b(x, y), \qquad (x, y) \in \partial\Omega. \tag{3.3}$$

$\mathbf{u}_b$ must satisfy

$$\int_{\partial\Omega} \mathbf{u}_b \cdot \mathbf{n} dS = 0, \tag{3.4}$$

where $\mathbf{n}$ is the outer unit normal to $\partial\Omega$. It is well known that we need not prescribe the boundary condition on p.

Much of the work done before using primitive varialbes on this problem begins with replacing Eqs. (3.1) and (3.2) by the system

$$-\mu\Delta\mathbf{u} + \nabla p = \mathbf{f}$$

$$\Delta p = \nabla \cdot \mathbf{f}$$

and then trying to solve the Laplace equation for p. The lack of boundary condition on p causes some difficulty. Much work has been done to determine the correct boundary condition for p (see, e.g., discussion in [35]). Work using the original system (3.1) and (3.2) has also been done, but it still requires some additional conditions for p near the boundary ([20], [35]).

Chorin ([11]) proposed a projection method for the more general Navier-Stokes equations that determines p without any artificial conditions on p. The method is based on the use of the equation $\nabla \cdot \mathbf{u} = 0$ instead of $\Delta p = \nabla \cdot \mathbf{f}$ to find p. Here we present a method based on the evaluation of p for the Stokes equations that requires no artificial conditions on p either. The idea is to use consistent finite difference operators to discretize Eqs. (1) and (2). It will be shown later in this section that the resulting system of equations is semi-definite if the difference operators satisfy a discrete analogue of the condition $(\mathbf{u}, \nabla p) = -(\nabla \cdot \mathbf{u}, p)$ (note that this condition only holds true when the boundary condition on the velocity is zero or periodic; see [12] for the discrete form of this condition). We eliminate $\mathbf{u}$ to form an equation $Ap = b$ which uniquely determines p (up to a constant, of course). Since it is computationally inefficient to express $\mathbf{u}$ in terms of p explicitly, we shall only have to evaluate Ap, i.e. given a p, we can find Ap, where A is not written out (as in the iterative implementation of Chorin's projection method ([11])). It turns out that for some properly chosen operators the matrix A is semi-positive definite and very well conditioned on the orthogonal complement of its null space, i.e. the condition number is close to 1 and bounded independently of the mesh size, so we can use the conjugate-gradient method to get the solution for p. Similar ideas were used by Maday and Patera ([28]) with a spectral element approach.

Assume the domain Ω is covered by some uniform grid of mesh size h. Following the notations of Anderson (1989), we approximate Eqs. (3.1) and (3.2) by finite difference equations,

$$-\mu\Delta_h\mathbf{u} + (\nabla_x^h, \nabla_y^h)p = \mathbf{f}, \tag{3.5}$$

$$D_x^h u + D_y^h v = 0, \tag{3.6}$$

where Δ_h is an approximation to the Laplacian, ∇_x^h and ∇_y^h to the derivatives in the gradient operator, D_x^h and D_y^h to the derivatives in the divergence operator. Notice that near the boundary $\Delta_h\mathbf{u}$ and $D_x^h u + D_y^h v$ contain velocity values on the boundary which are known. If we move those known terms to the right hand side of equations, we can rewrite Eqs. (3.5) and (3.6) as

$$-\mu\tilde{\Delta}_h\mathbf{u} + (\nabla_x^h, \nabla_y^h)p = \mathbf{f} + \mathbf{g}(\mathbf{u}_b) \tag{3.7}$$

$$\tilde{D}_x^h u + \tilde{D}_y^h v = h(\mathbf{u}_b) \tag{3.8}$$

where

$$\mathbf{g}(\mathbf{u}_b) = \mu\Delta_h\mathbf{u} - \mu\tilde{\Delta}_h\mathbf{u}$$

and

$$h(\mathbf{u}_b) = \tilde{D}_x^h u + \tilde{D}_y^h v - (D_x^h u + D_y^h v).$$

In other words, the operators with tilde's differ from the original operators only near the boundary, and they are the parts of the operators Δ_h, D_x^h, D_y^h that operate only on unknown values of the velocity. We will show how to calculate them once Δ_h, D_x^h, and D_y^h are defined in section (3.2) (see also [1]).

Put Eqs. (3.7) and (3.8) in block matrix form. We have

$$\begin{pmatrix} -\mu\tilde{\Delta}_h & 0 & \nabla_x^h \\ 0 & -\mu\tilde{\Delta}_h & \nabla_y^h \\ \tilde{D}_x^h & \tilde{D}_y^h & 0 \end{pmatrix} \begin{pmatrix} u \\ v \\ p \end{pmatrix} = \begin{pmatrix} f_x + g_x(\mathbf{u}_b) \\ f_y + g_y(\mathbf{u}_b) \\ h(\mathbf{u}_b) \end{pmatrix} \tag{3.9}$$

Consider the quadratic form

$$(u,v,p)\begin{pmatrix} -\mu\tilde{\Delta}_h & 0 & \nabla_x^h \\ 0 & -\mu\tilde{\Delta}_h & \nabla_y^h \\ \tilde{D}_x^h & \tilde{D}_y^h & 0 \end{pmatrix}\begin{pmatrix} u \\ v \\ p \end{pmatrix}$$

$$= -\mu[(u,\tilde{\Delta}_h u)+(v,\tilde{\Delta}_h v)]+(u,\nabla_x^h p)+(v,\nabla_y^h p)+(\tilde{D}_x^h u,p)+(\tilde{D}_y^h v,p).$$

It is positive semi-definite provided

$$(u,\nabla_x^h p)+(v,\nabla_y^h p) = -((\tilde{D}_x^h u,p)+(\tilde{D}_y^h v,p)) \tag{3.10}$$

and

$$(u,\tilde{\Delta}_h u)\le 0, \quad (v,\tilde{\Delta}_h v)\le 0 \tag{3.11}$$

Conditions (3.11) are satisfied for most reasonable difference approximations to the Laplacian while condition (3.10) is just a discrete analogue of the condition $(\mathbf{u},\nabla p) = -(\nabla\cdot\mathbf{u},p)$.

We can formally eliminate u and v in Eq. (9) to form a equation for p as follows: From Eq. (3.7) we obtain

$$u = \frac{1}{\mu}\{\tilde{\Delta}_h^{-1}\nabla_x^h p - \tilde{\Delta}_h^{-1}(f_x + g_x(\mathbf{u}_b))\}$$

and

$$v = \frac{1}{\mu}\{\tilde{\Delta}_h^{-1}\nabla_y^h p - \tilde{\Delta}_h^{-1}(f_y + g_y(\mathbf{u}_b))\}$$

Substitution of these expressions into Eq. (8) gives

$$(\tilde{D}_x^h\tilde{\Delta}_h^{-1}\nabla_x^h + \tilde{D}_y^h\tilde{\Delta}_h^{-1}\nabla_y^h)p$$
$$= \tilde{D}_x^h\tilde{\Delta}_h^{-1}(f_x + g_x(\mathbf{u}_b)) + \tilde{D}_y^h\tilde{\Delta}_h^{-1}(f_y + g_y(\mathbf{u}_b)) + \mu h(\mathbf{u}_b)$$

or simply

$$Ap = F^1 + F^2 \tag{3.12}$$

where

$$A = \tilde{D}_x^h \tilde{\Delta}_h^{-1} \nabla_x^h + \tilde{D}_y^h \tilde{\Delta}_h^{-1} \nabla_y^h \tag{3.13}$$

$$F^1 = \tilde{D}_x^h \tilde{\Delta}_h^{-1}(f_x + g_x(\mathbf{u}_b)) + \tilde{D}_y^h \tilde{\Delta}_h^{-1}(f_y + g_y(\mathbf{u}_b))$$

$$F^2 = \mu h(\mathbf{u}_b)$$

If we can solve Eq. (3.12) for p, then we can use Eq. (3.7) to obtain solutions for u and v.

Of course we do not have to find $\tilde{\Delta}_h^{-1}$ explicitly, but rather given a p (and $\mathbf{u}_b$), we can solve Eq. (3.7) for u and v then use Eq. (3.8) to form Ap. It turns out that for some properly chosen operators Δ_h, D_x^h, D_y^h, ∇_x^h and ∇_y^h the matrix A is semi-positive definite, so we can use the conjugate-gradient method to solve Eq. (3.12).

Recall that $\tilde{\Delta}_h$, $\tilde{D}_x^h$, $\tilde{D}_y^h$ are different from Δ_h, D_x^h, D_y^h only near the boundary, so if we choose

$$\Delta_h = D_x^h \nabla_x^h + D_y^h \nabla_y^h \tag{3.14}$$

which is just a discrete analogue of the definition of Laplacian, then we will have

$$\tilde{\Delta}_h = \tilde{D}_x^h \nabla_x^h + \tilde{D}_y^h \nabla_y^h$$

on all grid points except those near the boundary. By looking at the structure of matrix A in (3.13), it is reasonable to believe that A is close to the identity matrix, and that the conjugate-gradient method will converge in a few steps. We shall see that this is indeed the case by numerical examples.

3.2 Discretization of the Domain and Choice of D^h, ∇^h, Δ_h

We now implement the method for a special case of a staggered grid. Assume Ω is a unit square. Let $h = 1/n$. Define meshes (see Fig. 3.1)

$$U = \{(ih, (j + \frac{1}{2})h) \mid i = 0, ..., n; j = 0, ..., n-1\}$$

$$V = \{((i + \frac{1}{2})h, jh) \mid i = 0, ..., n-1; j = 0, ..., n\}$$

$$P = \{((i+\frac{1}{2})h, (j+\frac{1}{2})h) \mid i,j = 0,...,n-1\}$$

$$U^0 = U - U \cap \partial\Omega \qquad V^0 = V - V \cap \partial\Omega$$

and define u on U, v on V and p on P.

The operators are defined as follows:

$D_x^h: \ U \to P \ \ by \ (D_x^h u)_{i+\frac{1}{2},j+\frac{1}{2}} = (u_{i+1,j+\frac{1}{2}} - u_{i,j+\frac{1}{2}}) \ / \ h$

$D_y^h: \ V \to P \ \ by \ (D_y^h v)_{i+\frac{1}{2},j+\frac{1}{2}} = (v_{i+\frac{1}{2},j+1} - v_{i+\frac{1}{2},j}) \ / \ h$

$\nabla_x^h: \ P \to U^0 \ \ by \ (\nabla_x^h p)_{i,j+\frac{1}{2}} = (p_{i+\frac{1}{2},j+\frac{1}{2}} - p_{i-\frac{1}{2},j+\frac{1}{2}}) \ / \ h$

$\nabla_y^h: \ P \to V^0 \ \ by \ (\nabla_y^h p)_{i,j+\frac{1}{2}} = (p_{i+\frac{1}{2},j+\frac{1}{2}} - p_{i+\frac{1}{2},j-\frac{1}{2}}) \ / \ h$

and we define $\Delta_h u$ on U_0, $\Delta_h v$ on V_0 by the standard five point approximation to Laplacian except near the boundary where we use a first order approximation, for instance, we put

$$\frac{\partial^2 u}{\partial y^2} \approx \frac{u_{i,\frac{3}{2}} - 3u_{i,\frac{1}{2}} + 2u_{1,0}}{h^2}$$

at $j = 1$. Similarly for $j = n$ and $\frac{\partial^2 v}{\partial x^2}$. With those choices of the operators, it can be checked that relation (3.14) is satisfied on all grid points except those near the boundary.

Now the operators D^h etc. are defined. We can obtain the corresponding $\tilde{D}^h$ as follows: if $D_x^h u$ doesn't involve $\mathbf{u}_b$, put $\tilde{D}_x^h u = D_x^h u$; if it does, just put all $\mathbf{u}_b = 0$ in $D_x^h u$ to get $\tilde{D}_x^h u$. For instance

$$(\tilde{D}_x^h u)_{\frac{1}{2},j+\frac{1}{2}} = \frac{u_{1,j+\frac{1}{2}}}{h}.$$

If we define the inner product on U^0, V^0 and P by

$$(\phi,\psi)_{U^0} = \sum_{i=1}^{n-1}\sum_{j=1}^{n} \phi_{i,j-\frac{1}{2}}\psi_{i,j-\frac{1}{2}}$$

$$(\phi,\psi)_{V^0} = \sum_{i=1}^{n}\sum_{j=1}^{n-1} \phi_{i-\frac{1}{2},j}\psi_{i-\frac{1}{2},j}$$

and

$$(\phi,\psi)_P = \sum_{i=1}^{n}\sum_{j=1}^{n} \phi_{i-\frac{1}{2},j-\frac{1}{2}}\psi_{i-\frac{1}{2},j-\frac{1}{2}}$$

then it is easy to check that

$$(\tilde{D}_x^h u + \tilde{D}_y^h v, p)_P = -(\nabla_x^h p, u)_{U^0} - (\nabla_y^h p, v)_{V^0}.$$

Moreover, since

$$-\tilde{\Delta}_h = \begin{pmatrix} 5 & -1 & & & & -1 & 0 & -1 & & \\ -1 & 4 & -1 & & & & -1 & 0 & -1 & \\ \cdot & \cdot & & & & & & \cdot & \cdot & \\ \cdot & \cdot & & & & & & \cdot & \cdot & \\ \cdot & \cdot & & & & & & \cdot & \cdot & \\ \cdot & \cdot & & & & & & \cdot & \cdot & \\ \cdot & \cdot & & & & & & \cdot & \cdot & \\ \cdot & \cdot & & & & & & \cdot & \cdot & \\ \cdot & \cdot & & & & & & \cdot & \cdot & \\ & & -1 & 0 & -1 & & & & -1 & 5 \end{pmatrix}$$

we have by Gerschgorin's theorem

$$-(u, \tilde{\Delta}_h u)_{U^0} \geq 0$$

and

$$-(v, \tilde{\Delta}_h v)_{V^0} \geq 0.$$

Thus the matrix in Eq. (9) is indeed semi-positive definite and our numerical experiment indicates that the matrix A is also semi-positive definite.

With the discretization and the choice of operators made here, Eq. (3.12) has a non-trivial null space which is a constant pressure field. For the equation to have a solution the right hand side must be orthogonal to the null space. In this case, this condition turns out to be

$$\sum_{i,j}(F_{i,j}^1 + F_{i,j}^2) = 0$$

It can be verified that it is always true that

$$\sum_{i,j} F^1_{i,j} = 0$$

The second part of the sum, $\sum_{i,j} F^2_{i,j}$, is just a midpoint rule approximation to the condition $\int_{\partial\Omega} \mathbf{u}_b \cdot \mathbf{n} dS = 0$ (see [1]).

The above description can be naturally extended to the three dimensional case and all the conclusions remain true.

3.3 Solution of the Equations

In this section, we specify the routines we used in our numerical examples. The goal is to solve Eq. (3.7) for **u** quickly with a given p. In the two dimensional case there is a fast solver for this equation, namely, the subroutine BLKTRI from the NCAR set of routines FISHPACK. In the three dimensional case, however, there is no fast solver available. We can apply the fast fourier transform (FFT) technique to reduce the problem to a two dimensional problem (see, e.g., [37]). For instance, consider the equation for u,

$$\mu \tilde{\Delta}_h u = \nabla^h_x p + f_x + g_x(\mathbf{u}_b).$$

The grid is defined by $x = (i-1)h, \;\; y = (j-0.5)h, \;\; z = (k-0.5)h$. We use FFT in the x-direction to reduce the problem to (n-1) two dimensional systems on the staggered grid $y = (j-0.5)h, \;\; z = (k-0.5)h$. Since u is specified on the boundary, only sine functions are needed in the FFT. For the resulting two dimensional systems, we use the subroutine HSTCRT from the NCAR set of routines FISHPACK.

To solve equation $Ap = b$, we use the standard conjugate-gradient method. Since there is a non-trivial null space, care must be taken to eliminate components in the null space. Let **c** denote the null vector of the matrix (which is a constant vector in this case) and $(\cdot,\cdot)$ the inner product on p defined in section (3.2). The conjugate-gradient method algorithm is as follows:

$$r^0 = b - Ap^0 \qquad p^0 \quad \textit{initial} \quad \textit{guess}$$

For k = 0, 1, 2, $\cdots$

$$r^k = r^k - \frac{(r^k, \mathbf{c})}{(\mathbf{c}, \mathbf{c})}\mathbf{c}$$

$$\beta^k = \frac{(r^k, r^k)}{(r^{k-1}, r^{k-1})} \qquad k \geq 1 \qquad \beta^0 = 0$$

$$z^k = r^k + \beta^k z^{k-1}$$

$$\alpha^k = \frac{(r^k, r^k)}{(z^k, Az^k)}$$

$$p^{k+1} = p^k + \alpha^k z^k$$

$$r^{k+1} = r^k - \alpha^k A z^k$$

The computational work in each iteration step of the conjugate-gradient method is done mostly to form Ap, everything else is just some vector products which requires labor of order $O(N)$ (where N is the number of points in the domain). The formation of Ap requires solutions to two Laplace equations in the two dimensional case or three Laplace equations in the three dimensional case where in both cases the cost is $O(N \log N)$. Our solution to the steady Stokes equations thus requires work of order $2MN \log N$ or $3MN \log N$ where M is the number of iterations in the conjugate-gradient method. We will see from our numerical examples that M is very small even for very large N in the three dimensional case.

We first give an example in the two dimensional case. As a test problem, we take $\mathbf{f} = (3\cos(x)\sin(y), -\sin(x)\cos(y))$, $\mu = 1$, $u_b = \cos(x)\sin(y)$, $v_b = -\sin(x)\cos(y)$ and $\Omega = \{x, y | 0 \leq x \leq 2\pi, 0 \leq y \leq \pi\}$. In this case the exact solution is known to be

$$u = \cos(x)\sin(y), \quad v = -\sin(x)\cos(y),$$
$$\frac{\partial p}{\partial x} = \cos(x)\sin(y), \quad \frac{\partial p}{\partial y} = \sin(x)\cos(y).$$

In table 3.1 we display the results of the calculation. We use the residual r of the pressure equation (3.12) as our computation criterion, i.e., the iteration stops when $max(r_{i,j})$ is less than 1×10^{-7}. We should mention that by our construction this residual is exactly the divergence of the velocity field, i.e., we have

$$r_{i,j} = (D_x^h u + D_y^h v)_{i,j}$$

Table 3.1: Numerical results in 2-D case

Grid size	20×10	40×20	80×40	160×80
Iterations	8	10	10	11
L^∞ norm of r	9.50×10^{-8}	8.84×10^{-9}	7.71×10^{-8}	9.06×10^{-8}
$e(u)$	1.21×10^{-3}	2.92×10^{-4}	7.23×10^{-5}	1.80×10^{-5}
$e(v)$	5.06×10^{-4}	1.17×10^{-4}	2.87×10^{-5}	7.13×10^{-6}
$e(p_x)$	2.07×10^{-2}	5.68×10^{-3}	1.48×10^{-3}	3.77×10^{-4}
$e(p_y)$	1.49×10^{-2}	4.58×10^{-3}	1.26×10^{-3}	3.30×10^{-4}

We denote by $e(u), e(v), e(p_x)$ and $e(p_y)$ the errors of u, v, p_x and p_y, i.e., the absolute value of the differences between the exact solutions and our numerical solutions, respectively. All the errors are measured in the L^∞ norm.

For the case of three dimensions, we choose the test problem to be:

$$u_b = \sin(x)\cos(y)\cos(2z)$$

$$v_b = \cos(x)\sin(y)\cos(2z)$$

$$w_b = -\cos(x)\cos(y)\sin(2z)$$

$$\mathbf{f} = (0, 0, -18\cos(x)\cos(y)\sin(2z))$$

$$\mu = 1, \quad and \;\; \Omega = \{x, y, z | 0 \le x \le \pi, 0 \le y \le \pi, 0 \le z \le \pi/2\}.$$

We also have the exact solution as:

$$u = \sin(x)\cos(y)\cos(2z)$$

$$v = \cos(x)\sin(y)\cos(2z)$$

$$w = -\cos(x)\cos(y)\sin(2z)$$

$$p = 6\cos(x)\cos(y)\cos(2z).$$

Table 3.2 shows our numerical results for this problem.

We can see from the numerical results that we achieved second order accuracy for the velocity in both cases despite the fact that we used a first order approximation for the Laplacian operator near the boundary. The calculation for the pressure is less accurate, which is expected. The number of iterations grows very slightly as the mesh size increases

Table 3.2: Numerical results in 3-D case

Grid size	20×20×10	40×40×20	80×80×40	160×160×80
Iterations	13	16	18	19
L^∞ norm of r	9.82×10^{-9}	1.48×10^{-8}	5.18×10^{-8}	8.47×10^{-8}
$e(u)$	9.47×10^{-3}	2.66×10^{-3}	7.07×10^{-4}	1.83×10^{-4}
$e(v)$	9.47×10^{-3}	2.66×10^{-3}	7.07×10^{-4}	1.83×10^{-4}
$e(w)$	1.02×10^{-2}	2.64×10^{-3}	6.66×10^{-4}	1.67×10^{-4}
$e(p_x)$	0.105	5.54×10^{-2}	2.81×10^{-2}	1.41×10^{-2}
$e(p_y)$	0.105	5.54×10^{-2}	3.72×10^{-2}	1.41×10^{-2}
$e(p_z)$	0.202	0.100	6.71×10^{-2}	2.52×10^{-2}

both in the two and three dimensional cases. There is no substantial increase of the number of iterations from two dimensions to three dimensions. This makes our method particularly suitable for three dimensional calculations.

One should note that for the conjugate-gradient method to converge in a few iterations, it is very important that relation (3.14) in section (3.2) be satisfied, i.e. the gradient and divergence operators should combine to form the discrete Laplacian used in the discretization of $\Delta_h \mathbf{u}$. To show the importance of this, we make another calculation with a different discretization of the domain and different choices of the operators. We take the same test problem in two dimensions. This time the two components of the velocity are defined on the same set of grid points defined by $x, y = ih, i = 0, ..., n$. The pressure p is defined on the same grid as before. The operators are defined as:

$$(D_x^h u)_{i+\frac{1}{2},j+\frac{1}{2}} = \frac{1}{2h}[(u_{i+1,j+1} - u_{i,j+1}) + (u_{i+1,j} - u_{i,j})]$$

$$(D_y^h v)_{i+\frac{1}{2},j+\frac{1}{2}} = \frac{1}{2h}[(v_{i+1,j+1} - v_{i+1,j}) + (v_{i,j+1} - v_{i,j})]$$

$$(\nabla_x^h p)_{i,j} = \frac{1}{2h}[(p_{i+\frac{1}{2},j+\frac{1}{2}} - p_{i-\frac{1}{2},j+\frac{1}{2}}) + (p_{i+\frac{1}{2},j-\frac{1}{2}} - p_{i-\frac{1}{2},j-\frac{1}{2}})]$$

$$(\nabla_y^h p)_{i,j} = \frac{1}{2h}[(p_{i+\frac{1}{2},j+\frac{1}{2}} - p_{i+\frac{1}{2},j-\frac{1}{2}}) + (p_{i-\frac{1}{2},j+\frac{1}{2}} - p_{i-\frac{1}{2},j-\frac{1}{2}})]$$

and Δ_h by the standard five point approximation to Laplacian. These definitions satisfy (3.10) (see [33]) and (3.11) but not (3.14).

Table 3.3 shows the results of this calculation. We see that it requires about four times the iterations needed for the previous one.

Table 3.3: Iterations needed for a different discretization

Grid size	20×10	40×20	80×40	160×80
Iterations	31	45	48	49
L^∞ norm of r	7.98×10^{-8}	9.49×10^{-8}	9.12×10^{-8}	9.25×10^{-8}

3.4 Other Boundary Conditions

The method can be easily applied to problems with other boundary conditions such as periodic or Neumann boundary conditions or any combination of those, as long as the boundary conditions are properly prescribed so that the given Stokes problem has a unique solution and the Poisson equation (3.7) can be solved with the prescribed boundary condition on the velocity $\mathbf{u}$. We look in some detail to a 2 dimensional problem with a periodic condition in the x direction and a Dirichlet condition in y. First we claim that periodic condition alone does not determine the solution uniquely. This can be easily shown by the example where we have zero velocity boundary condition in y. Any parabolic flow in x direction will satisfy the Stokes equation and the given boundary conditions. But if we specify the pressure difference in x direction then the solution is uniquely determined. One also has to be careful that it is the pressure gradient that is periodic, instead of pressure itself. We can show however that the pressure is periodic except for an additive constant. Assume L is the length of domain in x direction, then for any x we have

$$\begin{aligned} p(x+L) &= \int_x^{x+L} \frac{\partial p}{\partial x}\, dx + p(x) \\ &= \int_0^{L} \frac{\partial p}{\partial x}\, dx + p(x) \\ &= A + p(x) \end{aligned} \tag{3.15}$$

where the constant A should be given for the problem to have a unique solution.

We discretize the domain as we did before for the Dirichlet boundary condition. Since now the velocity at the x boundary in unknown, we also need to establish Eq. (3.5) at the boundary, say for $i = n$ (see 3.1). This will require us to evaluate $(\nabla_x^h p)_{n,j+\frac{1}{2}}$. By Eq. (3.15), we define

$$\begin{aligned} (\nabla_x^h p)_{n,j+\frac{1}{2}} &= \frac{(p_{n+\frac{1}{2},j+\frac{1}{2}} - p_{i-\frac{1}{2},j+\frac{1}{2}})}{h} \\ &= \frac{(p_{\frac{1}{2},j+\frac{1}{2}} + A - p_{n-\frac{1}{2},j+\frac{1}{2}})}{h} \end{aligned}$$

Table 3.4: Numerical results in 3-D case for periodic conditions

Grid size	20×20×10	40×40×20	80×80×40	160×160×80
Iterations	8	8	2	2
L^∞ norm of r	1.68×10^{-8}	1.16×10^{-8}	3.45×10^{-12}	9.41×10^{-12}
$e(u)$	2.24×10^{-2}	5.62×10^{-3}	1.38×10^{-3}	3.45×10^{-4}
$e(v)$	2.21×10^{-2}	5.52×10^{-3}	1.38×10^{-3}	3.45×10^{-4}
$e(w)$	6.72×10^{-2}	1.70×10^{-2}	4.20×10^{-3}	1.05×10^{-3}
$e(p_x)$	7.60×10^{-2}	2.30×10^{-2}	5.93×10^{-3}	1.54×10^{-3}
$e(p_y)$	7.03×10^{-2}	2.16×10^{-2}	5.93×10^{-3}	1.54×10^{-3}
$e(p_z)$	0.131	3.32×10^{-2}	8.15×10^{-3}	2.04×10^{-3}

$$= \frac{(p_{\frac{1}{2},j+\frac{1}{2}} - p_{n-\frac{1}{2},j+\frac{1}{2}})}{h} + \frac{A}{h}$$

As for the velocity components, whenever $u_{n+1,\cdot}$ is needed, it is replaced by $u_{1,\cdot}$, and similarly for v. Those are the only changes that have to be made to accommodate the periodic boundary condition.

For later use in chapter 4, we choose a 3 dimensional problem as our numerical example. We use the same problem as we did before for Dirichlet boundary condition, but this time the boundary conditions in x and y directions are assumed to be periodic, and the z boundary condition remains of Dirichlet type. The domain Ω is chosen as

$$\Omega = \{x, y, z | 0 \leq x \leq 2\pi, 0 \leq y \leq 2\pi, 0 \leq z \leq \pi\}.$$

In this case the pressure is also periodic, so the constant A is zero for both x and y directions. The results of this computation are displayed in table 3.4.

From the results we see that in this case fewer iteration steps is needed for the method to converge and the solution is more accurate (remember that the domain is twice as large as that in section 3.3). We achieve second order accuracy for the pressure gradient as well as the velocity. We also notice that for grid size 80 × 80 × 40 and 160 × 160 × 80, the method only need 2 steps to converge. In both cases, the residuals go down to about order of 1 after one iteration, then the residuals go down all the way to about 10^{-12}, which is close to our machine accuracy, after the second iteration. This means that in those cases the matrix A is very close to the identity matrix.

In summary, we have presented a fast numerical technique for solving the steady-state Stokes equations which requires no artificial conditions for the pressure near the bound-

ary. Our numerical experiments show that the method is of second order accuracy for the velocity. The key idea of the method is to use some consistent difference operators to approximate the Stokes equations and then derive a equation $Ap = b$ for the pressure such that the matrix A is semi-positive definite and very well conditioned on the orthogonal complement of its null space. Therefore it is very efficient to use the standard conjugate-gradient method to solve the pressure equation. We implemented our method on a staggered grid for rectangular (cubic) domains and showed that the conjugate-gradient method converged in a very few iterations even for a very large number of grid points in the three dimensional case. The reason we chose a staggered grid is because it is the simplest way to define the gradient and divergence operators so that they combine to form the usual 5 point Laplacian. Thus it becomes easy to solve the Poisson equation for a given p. Other discretization will also work as long as relation (3.14) in section (3.2) is satisfied and the resulting Poisson equation is easy to solve. The method can also be extended to other boundary conditions very easily since the boundary conditions come in only in the solutions of the Poisson equation. Finally, the method is certainly applicable to more general domains as long as we can solve the Laplace equation on those domains.

Chapter 4

Stokes Flows in Bounded Domains and Evaluation of Effective Viscosity

4.1 Introduction

In this chapter, we apply the method of reflections to problems with bounded domains by treating the boundary of the domain in a similar way we treated the sphere, in the sense that when the given boundary condition is not satisfied, we just find a velocity field inside the domain to satisfy the given condition, ignore the existence of spheres inside. Assume we have a box C with fluid and spheres $B_1, B_2, \ldots, B_n$ inside the box at positions $\vec{x}_i, i = 1, \ldots, n$. We are given the boundary conditions on the boundary of the box,

$$\vec{u}|_{\partial C} = \vec{U}_b$$

and the motions of spheres,

$$\vec{U}_{B_1}, \vec{U}_{B_2}, \ldots, \vec{U}_{B_n}, \vec{\Omega}_{B_1}, \vec{\Omega}_{B_2}, \ldots, \vec{\Omega}_{B_n}.$$

Using the method described in chapter 3, we find a velocity field $\vec{u}_C^0$ in C that satisfies the given boundary condition, as if there were no spheres inside. Then we can use the method of reflections to do one step of iteration through all the spheres as if we had an unbounded domain in the following way:

We first find $\vec{u}^0_{B_1}$ such that

$$\vec{u}^1_{B_1} = -\vec{u}^0_C + \vec{U}_1 + (\vec{x} - \vec{x}_1) \times \vec{\Omega}_1 \quad on \quad \partial B_1$$

so

$$\vec{u}^0_C + \vec{u}^0_{B_1} = \vec{U}_1 + (\vec{x} - \vec{x}_1) \times \vec{\Omega}_1$$

on ∂B_1. Then we find $\vec{u}^1_{B_2}$ so that

$$\vec{u}^1_{B_2} = -\vec{u}^0_C + \vec{U}_2 + (\vec{x} - \vec{x}_2) \times \vec{\Omega}_2 - \vec{u}^1_{B_1} \quad on \quad \partial B_2,$$

$$\ldots \quad \ldots \quad \ldots$$

and $\vec{u}^1_{B_n}$ such that

$$\vec{u}^1_{B_n} = -\vec{u}^0_C + \vec{U}_n + (\vec{x} - \vec{x}_n) \times \vec{\Omega}_n - \sum_{j=1}^{n-1} \vec{u}^1_{B_j} \quad on \quad \partial B_n.$$

This will generate a velocity field

$$\vec{u}^1_B = \vec{u}^1_{B_1} + \vec{u}^1_{B_2} + \ldots + \vec{u}^1_{B_n}.$$

We take

$$\vec{u}^0 = \vec{u}^0_C + \vec{u}^0_B$$

as our new velocity field. Of course generally

$$\vec{u}_B|_{\partial C} \neq 0$$

so the boundary condition for the box is no longer satisfied. We then find another $\vec{u}^1_C$ in C such that

$$\vec{u}^1_C|_{\partial C} = -\vec{u}^0_B|_{\partial C}$$

and set

$$\vec{u}^1 = \vec{u}^0 + \vec{u}^1_C = \vec{u}^0_C + \vec{u}^0_B + \vec{u}^1_C.$$

We then have

$$\vec{u}^1|_{\partial C} = \vec{u}^0_C|_{\partial C} + \vec{u}^0_B|_{\partial C} + \vec{u}^1_C|_{\partial C} = \vec{u}^0_C|_{\partial C} = \vec{U}_b.$$

Thus we complete one step of iteration. If the iteration converges, it is obvious that the limit velocity field will satisfy the no slip condition on the surfaces of all the spheres and the given condition on the boundary of the box. When the characteristic distance from the

Table 4.1: Convergent rate for a sphere fixed in a box

Radius a	0.05	0.1	0.2	0.3	0.35	0.4	0.45
N	7	11	24	63	109	208	411
$\max(U_B^N), \times 10^{-5}$	5.031	4.746	9.325	8.436	8.222	9.615	9.790

spheres to the boundary of the box is large compared to the radii of the spheres, experience shows that this procedure will converge. As we will see later from the numerical examples we will have the convergence in many cases where the distance is not large. Unlike the situation in the unbounded domain, here we will not have the convergence for all the sphere configurations inside the box. One possible reason it is different here is that the Stokes flow inside a box is of the same order of magnitude as the given boundary value, whereas the Stokes flow outside a single sphere decays as $\frac{a}{r}$ where r is the distance from the point in consideration to the center of the sphere and a is the radius of the sphere.

4.2 Numerical examples

To see how the method converges in a bounded domain, we consider a number of sphere configurations inside a box. In all the examples, the box is defined by

$$C = \{x, y, z | \ 0 \leq x \leq 2, 0 \leq y, z \leq 1\}.$$

We assume there is a uniform flow through the box so the boundary conditions are given by

$$u|_{\partial C} = 1, \quad v|_{\partial C} = w|_{\partial C} = 0.$$

All the spheres are assumed to be fixed inside the box.

As a first example, we fix one sphere in the middle of the box. We vary the radius of the sphere to see how the convergence rate changes. In our computation, the iteration is stopped if $U_B^N \leq \epsilon = 10^{-4}$. The results are displayed in table 4.1 and the velocity field at $z = 0.5$ is shown in figure 4.1 for radius $a = 0.2$.

From the results we can see that when the radius of the sphere is less than 0.35 the method converges in a reasonable number of steps. When the radius is greater than 0.4 the method does not converge very well, but in that case the sphere is very large compared to the size of the box. We also ran the program for $a = 0.5$ in which case the sphere touches

Table 4.2: Convergent rate for two spheres fixed in a box

Radius a	0.05	0.1	0.2	0.3	0.35	0.4	0.45
N	7	12	32	92	167	326	645
$\max(\vec{u}_B^N)$,$\times 10^{-5}$	6.295	8.099	8.375	9.194	8.803	9.615	9.906

the box boundaries in two directions. In this case the velocity field U_B^n still gets smaller each step but very slowly. The method diverges for $a = 0.5$ when the length of the box in x direction is 1.25.

Next we look at some multi-sphere configurations inside the box. We first put two spheres of same size in the box at points $\vec{x}_1 = (0.5, 0.5, 0.5), \vec{x}_2 = (1.5, 0.5, 0.5)$. We change the radius of the sphere to see how the convergence of the method changes. Results of the calculation are shown in table 4.2 and the velocity field at $z = 0.5$ is shown in figure 4.2 for radius $a = 0.2$. We can see that when the radius is less than or equal to 0.1 the convergence rate is about the same as the case with one sphere. This means in those cases the interaction between the boundary and the spheres dominates the convergence rate. When the radius of the spheres is greater than or equal to 0.2 the interaction between the two spheres also come into effect.

Finally we apply the method to configurations with more than two spheres. Figure 4.3 shows the velocity field at $z = 0.5$ for three spheres of radius $a = 0.15$ located at $\vec{x}_1 = (0.5, 0.3, 0.5), \vec{x}_2 = (1.5, 0.3, 0.5)$ and $\vec{x}_3 = (0.5, 0.7, 0.5)$. The convergence is this case is obtained in 29 steps. When the radius $a = 0.2$ the steps needed is 52. Figure 4.4 and 4.5 shows the velocity field at $z = 0.5$ for five and seven spheres of radius $a = 0.15$ located at $\vec{x}_1 = (0.5, 0.3, 0.5), \vec{x}_2 = (1.5, 0.3, 0.5), \vec{x}_3 = (1.0, 0.3, 0.5), \vec{x}_4 = (0.75, 0.7, 0.5), \vec{x}_5 = (1.25, 0.7, 0.5)$ and $\vec{x}_6 = (0.25, 0.7, 0.5), \vec{x}_7 = (1.75, 0.7, 0.5)$. 46 and 61 steps are needed in those cases, respectively.

4.3 Application to the Evaluation of Effective Viscosity

In this section we apply the method of reflections to the calculation of effective viscosity of a dilute suspension of rigid spheres in a shear flow. In particle suspensions when the volume fraction of the particles is small the suspension can be considered as a homogeneous fluid on a macroscopic scale. The viscosity of that homogeneous fluid is called

the effective viscosity of the suspension. The earliest work on this was done by Einstein [14] where the following Einstein's formula for the viscosity of a dilute suspension with spherical particles was obtained:

$$\frac{\mu}{\mu_0} = 1 + 2.5\phi$$

where μ is the viscosity of the suspension, μ_0 the viscosity of the original fluid and ϕ the volume fraction of particles. Later work on this subject has been done by many people (see, e.g., [19], [2],[30], [13] and [40]) Here we try to use the method of reflections to evaluate the effective viscosity of a monolayered suspension of spheres in the $x - y$ directions and a shear flow condition in z direction. Since the method of reflections cannot deal with problems with infinitely many spheres we first approximate the problem by a model with one sphere suspended in the middle of a unit square box (see Fig. 4.6) and impose periodic boundary conditions in the $x - y$ directions when we solve for the velocity field $\vec{u}_C$. This model basically neglect the interaction between the spheres. Later on we will put two or more spheres in the box to take into account some of the interactions between spheres.

In the problem of suspensions, it is assumed that the spheres are suspended in the fluid in such a way that the force and torque on each sphere are zero. This can be achieved in the same way as discussed in chapter 2. In our computation, the boundary conditions are given as the follows,

$$\vec{u}_{z=0.5} = (+1, 0, 0), \quad \vec{u}_{z=-0.5} = (-1, 0, 0).$$

Let F and F_0 be the total shear force on the top and bottom plates ($z = 0.5$ and $z = -0.5$) with spheres and without spheres, respectively. We define the effective viscosity to be the ratio of F and F_0, i.e.

$$\frac{\mu}{\mu_0} = \frac{F}{F_0}.$$

There are some other definitions ([19] and [2]). The one we use here is easy to compute numerically. In our computation we fix the size of the box and vary the size of the sphere to change the volume fraction. The result of our computation is displayed in figure 4.7. The solid line is the Einstein's formula and the dots are our numerical results. We can see that only when the volume fractions are very small do our results agree well with Einstein's formula. When the volume fraction is large our results are larger than the results from Einstein's formula. This trend was also noticed in some other numerical computations and experimental results (see, e.g., [40]) only that here it occured too early. The reason for this is that we neglected the interaction between the spheres.

Next we put two spheres in the box (see Fig. 4.8) to take into account some of the interaction between spheres. The spheres are located at positions $\vec{x}_1 = (0.5, 0.25, 0.5), \vec{x}_2 = (0.5, 0.75, 0.5)$. The results of this computation is shown in figure 4.9. As we can see this time our numerical results agree very well with the Einstein's formula up to volume fraction $\phi = 0.1$.

Chapter 5

Discussion and Conclusion

We have presented a numerical study of Stokes flow with suspended spheres by the method of reflections. The method is based on the solution of the Stokes equations outside a single sphere and the linearity of the Stokes equations. We used a harmonic expansion to find the Stokes flow outside a single sphere. We constructed a iterative scheme to find the Stokes flow outside a number of spheres in an unbounded domain when the motions of spheres are given by reducing the problem to a series of solutions of Stokes equations outside a single sphere. Our numerical experiments suggested that the method is convergent for all sphere configurations in this case. We then extended the method to problems where the forces and torques on the spheres are given and applied the method to find the periodic solution of three sedimenting spheres. Our results agree very well with previous work done by Caflisch et al. [10] when the initial positions of the spheres are symmetric and show some interesting long time scale periodicity of the solution when the initial positions are asymmetric.

The version of the method of reflections we presented here is similar to the collocation technique of Ganatos *et al.* [15] in that the velocity field outside the spheres is expressed as a sum of a series of truncated harmonic expansions about the center of each sphere, and then numerical computations are used to determine the coefficients of the expansions. The difference is here we establish the linear system of equations for the coefficients of the expansions (which is done implicitly) by requiring that if we use the final resulting velocity field on the surface of each sphere to generate another truncated harmonic expansion around the center of that sphere, using the method of chapter 1, all the coefficients will be zero, instead of requiring the velocity to be zero at some discrete points on the surface of each sphere,

as done in the collocation method. The iterative procedure of the method of reflections can be seen as an iterative method to solve the resulting linear system of equations for the coefficients. Our method is thus comparable to the collocation technique in terms of accuracy, with the advantage of avoiding the oscillation of the velocity field in some cases of the collocation method. The cost is a bit more expensive since the linear system in our method is more expensive to establish, and the iterative procedure to solve the linear system could be more expensive also.

In an effort to extend the method to bounded domains, we developed a fast numerical algorithm for finding solutions of steady Stokes equations. The algorithm is based on the observation that when the finite difference operators approximating the divergence and gradient operators in the Stokes equations are chosen properly we can derive a linear system of equations for the pressure p which is semi-positive definite and very well conditioned on the orthogonal complement of its null space. The system can be easily solved using the conjugate-gradient method. With this algorithm, we extended the method of reflections to problems in a bounded domain by finding a reflection to satisfy the boundary condition on the boundary of the domain. Unlike the case of unbounded domains, the method diverges in this case for some sphere configurations. One way to overcome this problem is to require each reflection of spheres always satisfy the given boundary condition of the domain, as was done in the proof of Luke [27]. Unfortunately to find that reflection is not trivial. There is no known exact solution or easy way of numerical computation.

We applied the method of reflections in bounded domains to the evaluation of effective viscosity of sphere suspension in a shear flow. Our results showed good agreement with the Einstein's formula when the sphere volume fraction is small.

Our numerical results lead us to several conclusions about the method of reflections.

First and most importantly our numerical experiments suggested that the method is convergent for all sphere configurations in an unbounded domain. The distances between the spheres have much more effect on the rate of convergence than the number of spheres. The convergence of the method is slow when the spheres are very close to each other. The reason behind this is that when spheres are very close to each other, the effect of lubrication will dominate the interaction between the spheres and a lot of iterations will be needed to adequately represent this effect in the method of reflections. Thus the method is best used when the spheres are not very closed to each other. Otherwise it is better to use some

method that will explicitly take into account the lubrication effect (see, e.g., [13]).

Secondly, in the case of bounded domains the method converges slower than in unbounded domains because of the presence of the boundary of the domain. The method diverges for some sphere configurations but in most cases it does converge. The good agreement of our result for the effective viscosity with the Einstein formula shows that the method can yield good results for certain kinds of problems, for example problem in solving suspension. The largest sphere volume fraction in evaluating the effective viscosity using two spheres is achieved when the radius of the spheres $a = 0.25$. In that case the spheres are touching each other and touching the boundary of the domain in one direction. Our calculation gives a reasonable result even in this situation, showing that the method can be used even when the spheres are very close to each other and close to the boundary of the domain.

Finally the convergence of the method in unbounded domains depends on the fact that the Stokes flow outside a single sphere decays as $\frac{a}{r}$. This is true for particles of any shape, so for non-shperical particles if we can find the velocity field outside a single particle in some way then the same reflection procedure can be applied to obtain the velocity field outside a collection of such particles. The method should be applicable to other problems with a similar property, like finding the electro-magnetic field outside a number of particles (spheres).

Bibliography

[1] C. R. Anderson. Derivation and Solution of the Discrete Pressure Equations for the Incompressible Navier-Stokes Equations. Technical Report LBL-26353, Lawrence Berkeley Laboratory, Berkeley, CA, 1988.

[2] G. K. Batchelor. Transport properties of two-phase materials with random structure. *Annual Review of Fluid Mechanics*, 6:227, 1974.

[3] G. Bossis and J. F. Brady. Dynamic simulation of sheared suspension. I. General method. *J. Chem. Phys.*, 80:5141–5154, 1984.

[4] J. F. Brady and G. Bossis. Stokesian dynamics. *Annual Review of Fluid Mechanics*, 20:111–157, 1988.

[5] S. Broersma. Viscous Force Constant for a Closed Cylinder. *J. Chem. Phys.*, 32(6):1132–1135, 1960.

[6] S. Broersma. Rotational Diffusion Constant of a Cylindrical Particle. *J. Chem. Phys.*, 32(6):1126–1131, 1960.

[7] J. M. Burgers. *Amsterdam: North Holland Publishing Co.*, 1938.

[8] J. M. Burgers. *Proc. Konigl. Akad. Wetenschap. (Amsterdam)*, 44, 1941.

[9] J. M. Burgers. *Proc. Konigl. Akad. Wetenschap. (Amsterdam)*, 45, 1942.

[10] R. E. Caflisch, Luke Lim, C., J. H. C., and A. S. Sangani. Periodic solutions for three sedimenting spheres. *Phys. Fluids*, 31(11), November 1988.

[11] A. J. Chorin. Numerical Solution of the Navier-Stokes Equations. *Math. Comp.*, 22:745, 1968.

[12] A. J. Chorin. On the Convergence of Discrete Approximations to the Navier-Stokes Equations. *Math. Comp.*, 23:341, 1969.

[13] L. Durlofsky, J. F. Brady, and G. Bossis. Dynamic simulation of hydrodynamically interacting particles. *J. Fluid Mechanics*, 180:21–49, 1987.

[14] A. Einstein. *Investigations on the Theory of the Brownian Movement.* Dover, New York, 1956.

[15] P. Ganatos, R. Pfeffer, and S. Weinbaum. A numerical-solution technique for three-dimensional stokes flows, with application to the motion of strongly interacting spheres in a plane. *J. Fluid Mech.*, 84, 1978.

[16] M. J. Gluckman, R. Pfeffer, and S. Weinbaum. A new technique for treating multiparticle slow viscous flow: Axisymmetric flow past spheres and spheroids. *J. Fluid Mech.*, 50(4), 1971.

[17] M. J. Gluckman, R. Pfeffer, and S. Weinbaum. Axisymmetric slow viscous flow past an arbitrary convex body of revolution. *J. Fluid Mech.*, 55:677, 1972.

[18] A. J. Goldman, R. G. Cox, and H. Brenner. The slow motion of two identical arbitrary oriented spheres through a viscous fluid. *Chemical Engineering Science*, 21, 1966.

[19] J. Happel and H. Brenner. *Low Reynolds Number Hydrodynamics.* Noordhoff, second edition, 1973.

[20] F. H. Harlow and J. E. Welch. Numerical Calculation of Time-Dependent Viscous Incompressible Flow of Fluid with Free Surface. *Physics of Fluids*, 8:2182, 1965.

[21] Q. Hassonjee, P. Ganatos, and R. Pfeffer. A strong-interaction theory for the motion of arbitrary three-dimensional unidirectional flows. *J. Fluid Mech.*, 197, 1988.

[22] B. P. Ho and L. G. Leal. Inertial migration of rigid spheres in two-dimensional unidirectional flows. *J. Fluid Mech.*, 65:365, 1974.

[23] E. W. Hobson. *Spherical and Ellipsoidal Harmonics.* Chelsea Publishing Company, 1965.

[24] Wu-Yi Hsiang. On the density of sphere packing in E^3 -Kepler's conjecture and Hilbert's 18th problem. Technical Report PAM-516, University of California, Berkeley, CA, December 1990.

[25] G. J. Kynch. The slow motion of two or more spheres through a viscous fluid. *J. Fluid Mech.*, 5:193, 1959.

[26] H. Lamb. *Hydrodynamics.* Dover, six edition, 1945.

[27] J. H. C. Luke. Convergence of a multiple reflection method for calculating Stokes flow in a suspension. *SIAM J. Appl. Math.*, 49(6):1635–1651, 1989.

[28] Y. Maday and A. T. Patera. *Spectral Element Method for the Incompressible Navier-Stokes Equations.* in State-of-art Surveys on Computational Mechanics, A.K. Noor and J. T. Oden, ed. (ASME 1989).

[29] J. S. McNown and P. N. Lin. *Proc. Second Midwestern Conf. Fluid Mech.*, page 109, 1952.

[30] W. B. Russel. Review of the Role of Colloidal Forces in the Rheology of Suspensions. *J. Rheol.*, 24:287, 1980.

[31] M. Smoluchowski. *Bull Int. Acad. Polonaise Sci. Lett.*, 1A:28, 1911.

[32] M. Smoluchowski. *Proc. Fifth Int. Cong. Math.*, 2:192, 1912.

[33] A. B. Stephens, J. B. Bell, J. M. Solomon, and L. B. Hackerman. A finite Difference Galerkin Formulation for the Incompressible Navier-Stokes Equations. *J. Comp. Phys.*, 53:152, 1984.

[34] M. Stimson and G. B. Jeffery. *Proc. Roy. Soc.*, A111:110, 1926.

[35] J. Strikwerda. Finite difference methods for the Stokes and Navier-Stokes equations. *SIAM J. Sci. Stat. Comput.*, 5:56, 1984.

[36] A. M. Stroud and D. Secrest. *Gaussian Quadrature Formulas.* Prentice Hall, Englewood Cliffs, N. J., 1967.

[37] P. N. Swarztrauber. The method of cyclic reduction, Fourier analysis and the FACR algorithm for the discrete solution of Poisson's equation on a rectangle. *SIAM Review*, 19(3):490, 1977.

[38] C. K. W. Tam. The drag on a cloud of spherical particles in low Reynolds number flow. *J. Fluid Mech.*, 38:537, 1969.

[39] C. Tchen. Motion of Small Particles in Skew Shape Suspended in a Viscous Fluid. *J. Appl. Phys.*, 25:463, 1954.

[40] T. Tran-Cong, N. Phan-Thien, and A. L. Graham. Stokes problems of multiparticle system: Periodic arrays. *Physics of Fluids*, A 2(5):666, May 1990.

[41] S. Weindaum, P. Ganatos, and Zong-Yi Yan. Numerical multipole and boundary integral equation techniques in Stokes flow. *Annual Review of Fluid Mechanics*, 22:275–316, 1990.

[42] G. K. Youngren and A. Acrivos. Stokes flow past a particle of arbitary shape: a numerical method of solution. *J. Fluid Mechanics*, 69:377–403, 1975.

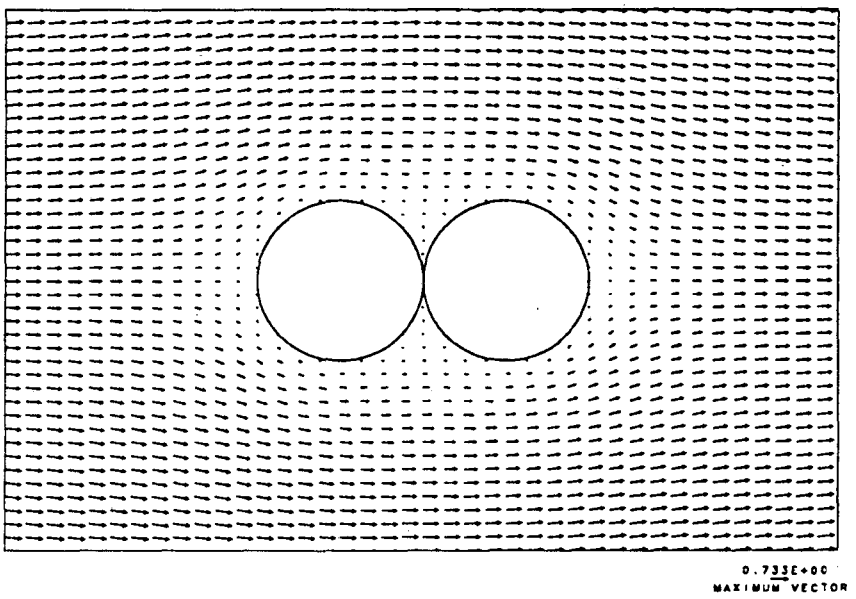

Figure 2.1: Velocity field of the two sphere problem

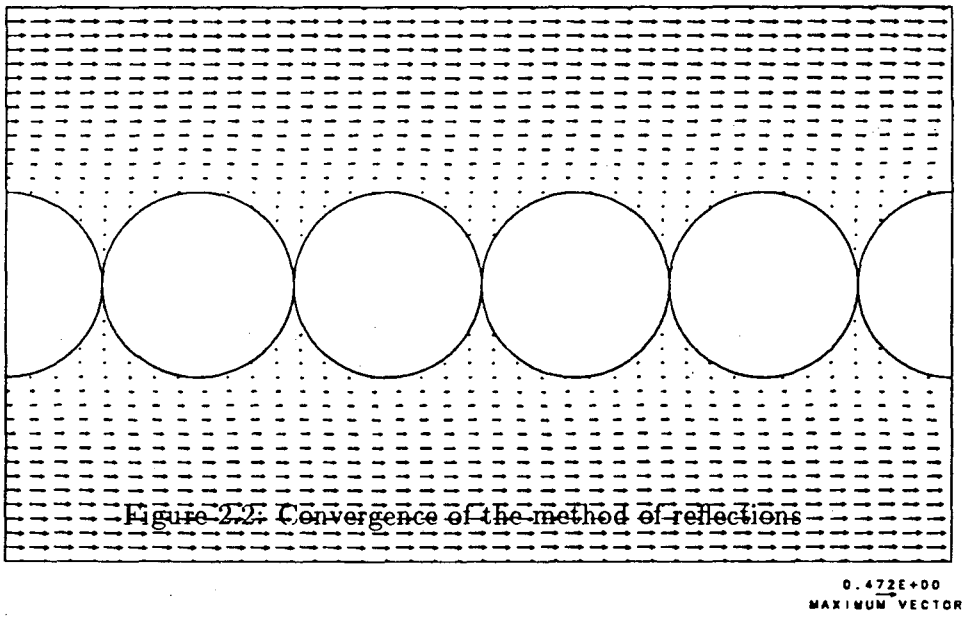

Figure 2.2: Convergence of the method of reflections

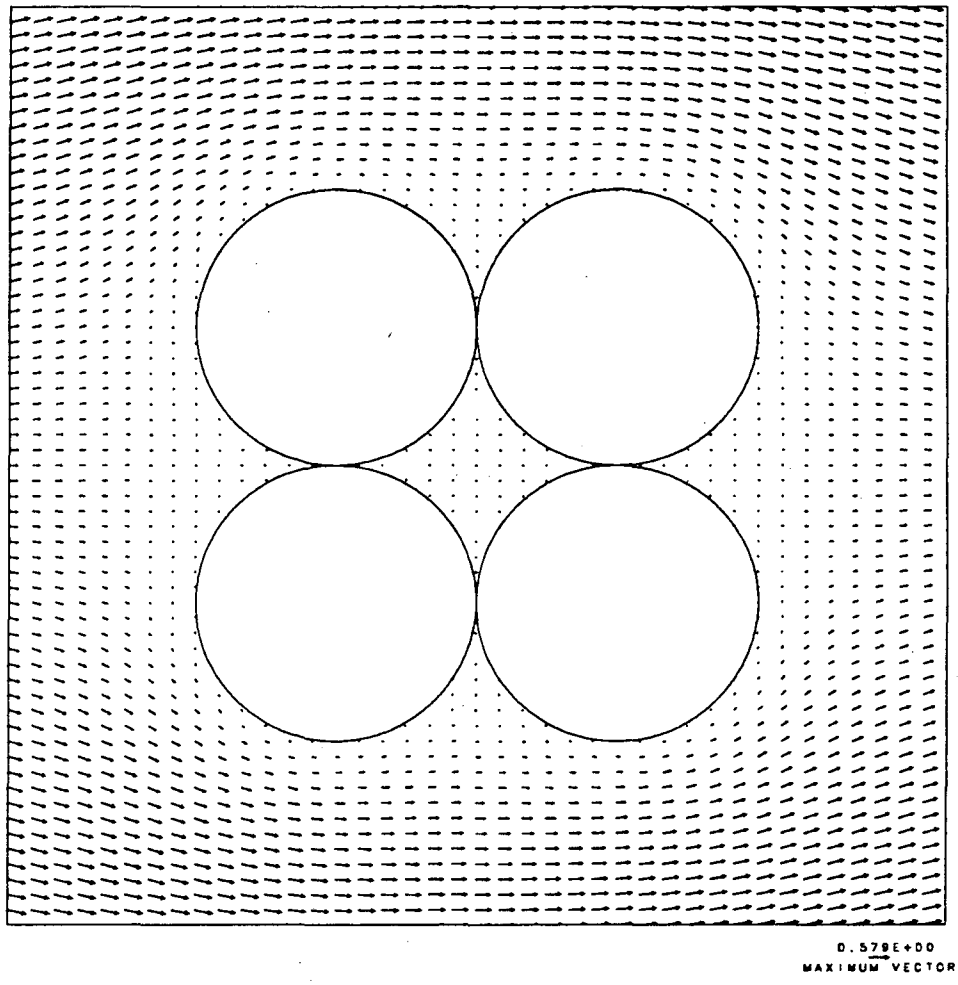

Figure 2.3: Velocity field of the 4 sphere configuration

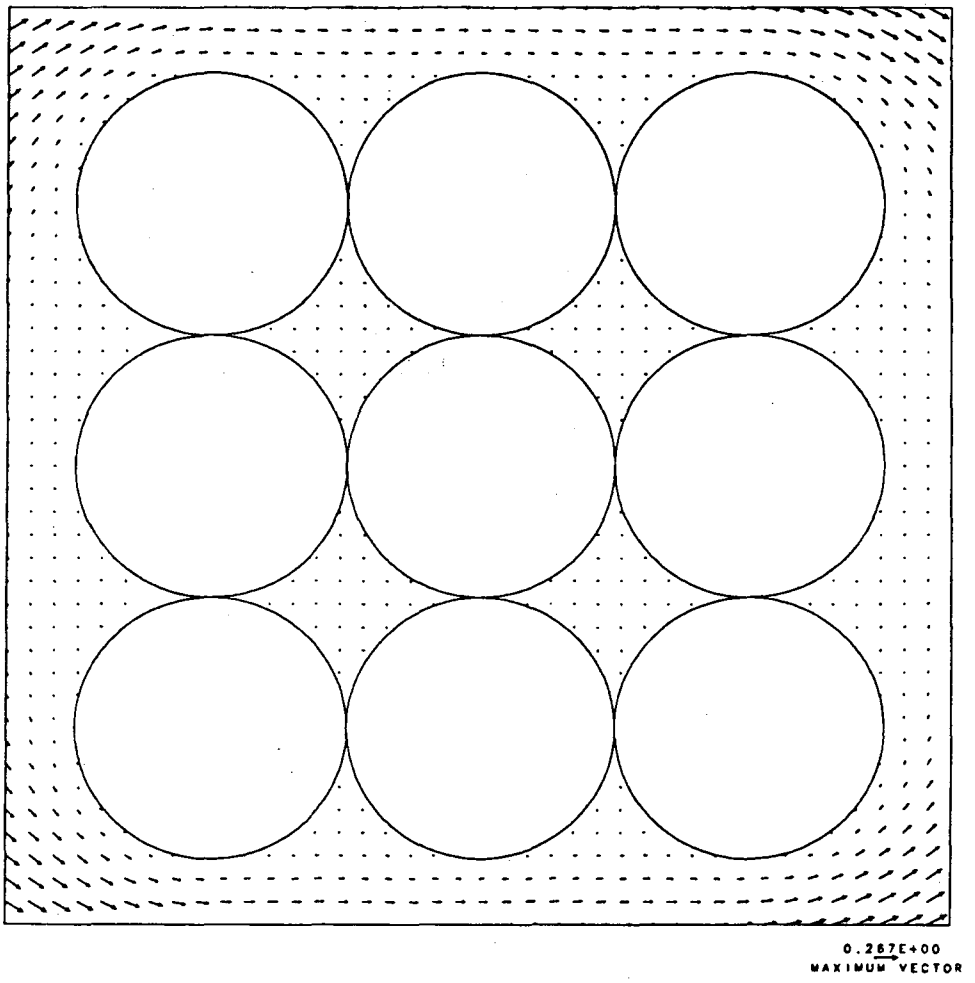

Figure 2.4: Velocity field of the 9 sphere configuration

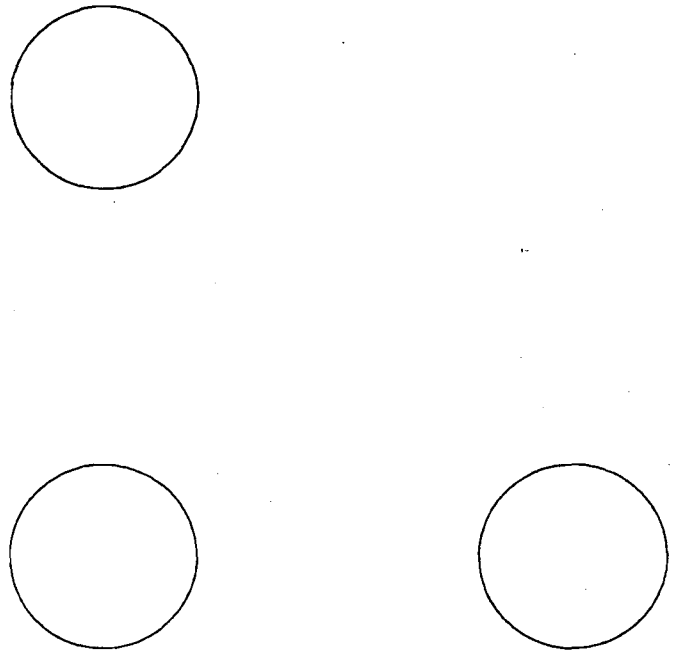

Figure 2.5: Three spheres falling down under gravity

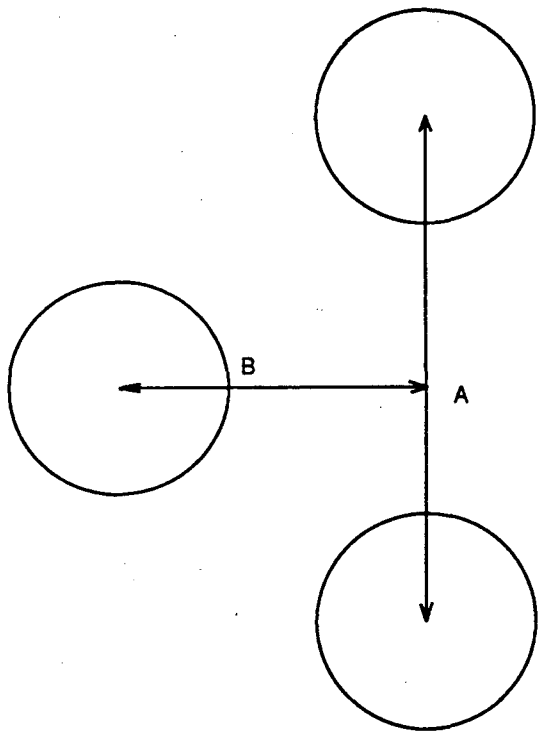

Figure 2.6: Symmetric initial position

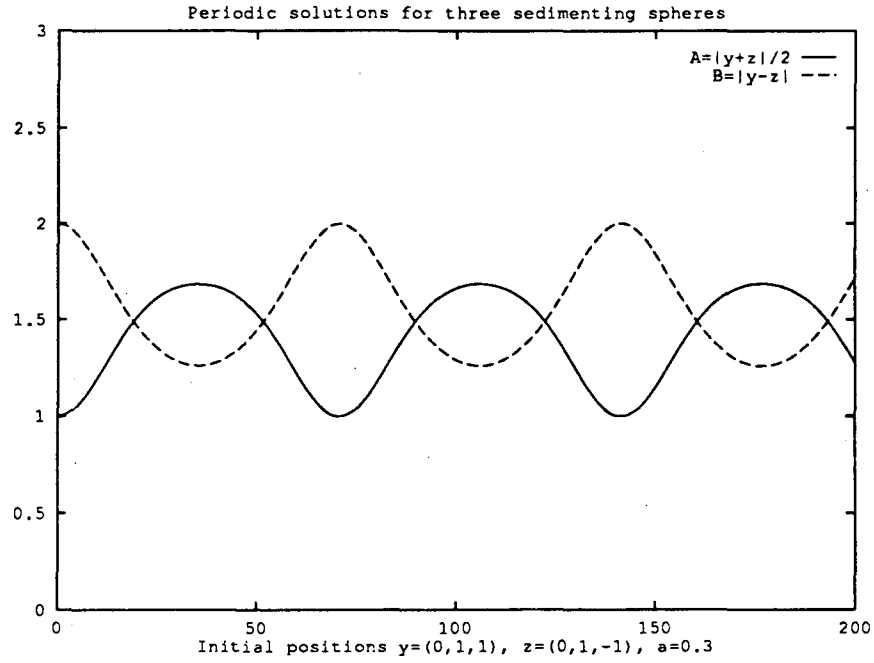

Figure 2.7: Symmetric initial position, result 1

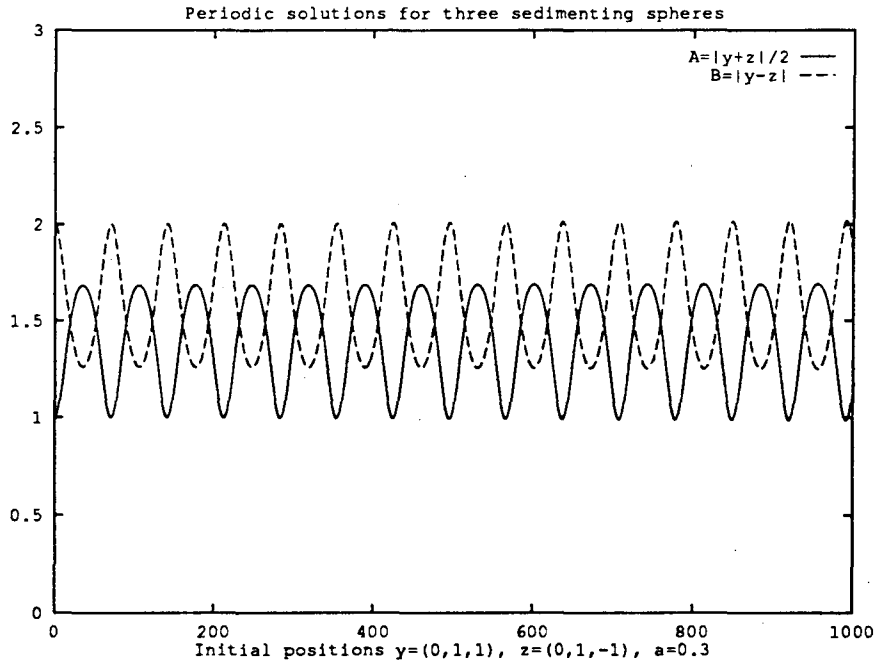

Figure 2.8: Symmetric initial position, result 2

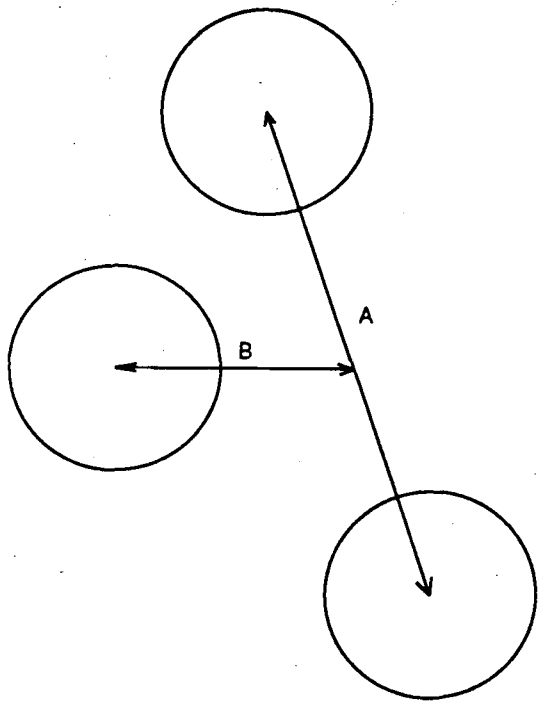

Figure 2.9: Asymmetric initial position

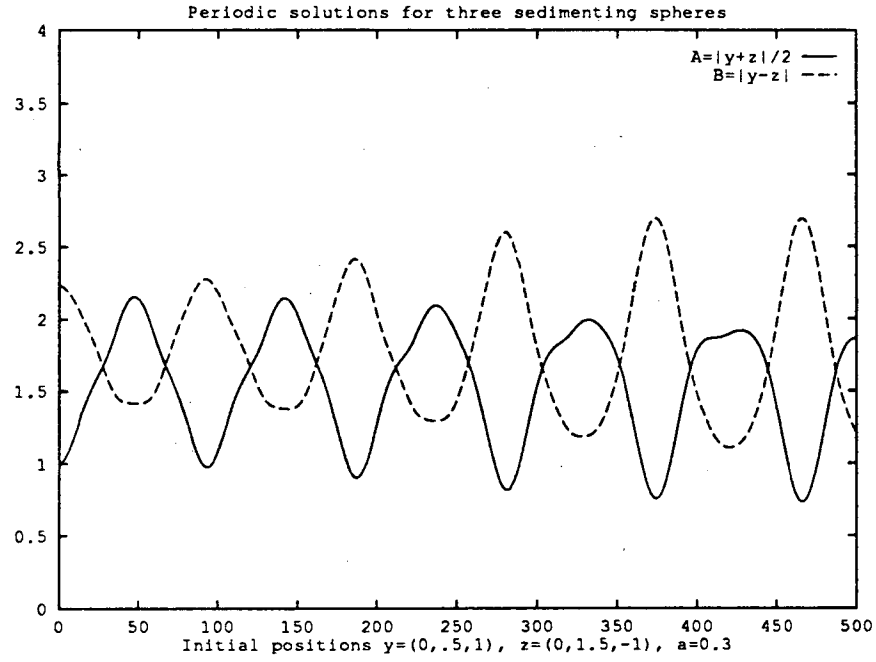

Figure 2.10: Asymmetric initial position, result 1

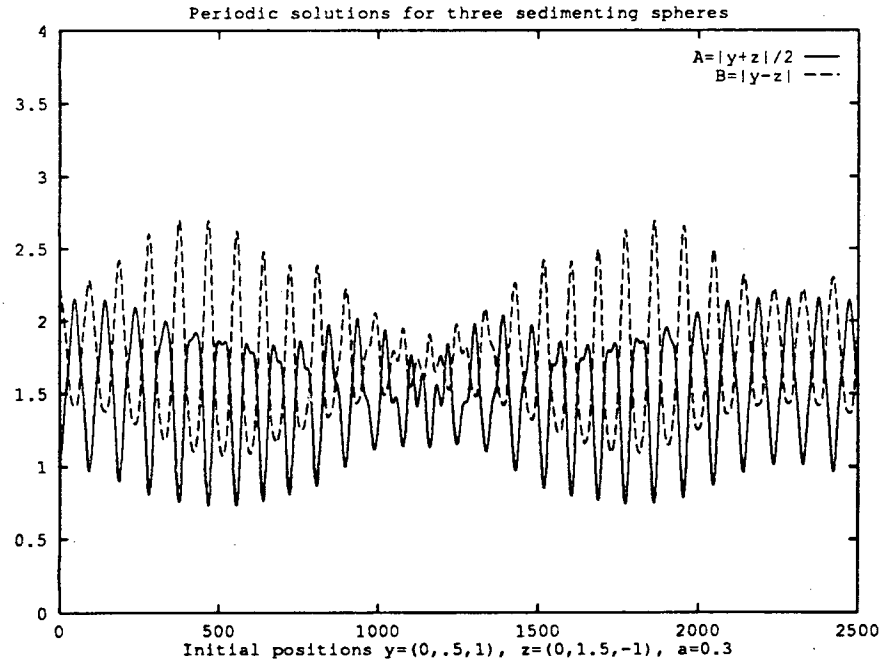

Figure 2.11: Asymmetric initial position, result 2

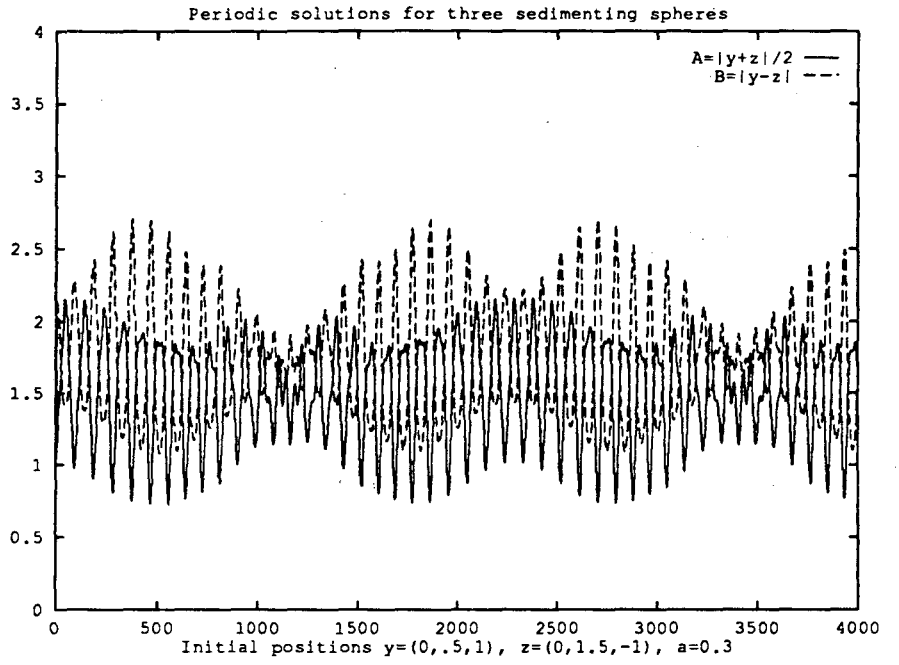

Figure 2.12: Asymmetric initial position, result 3

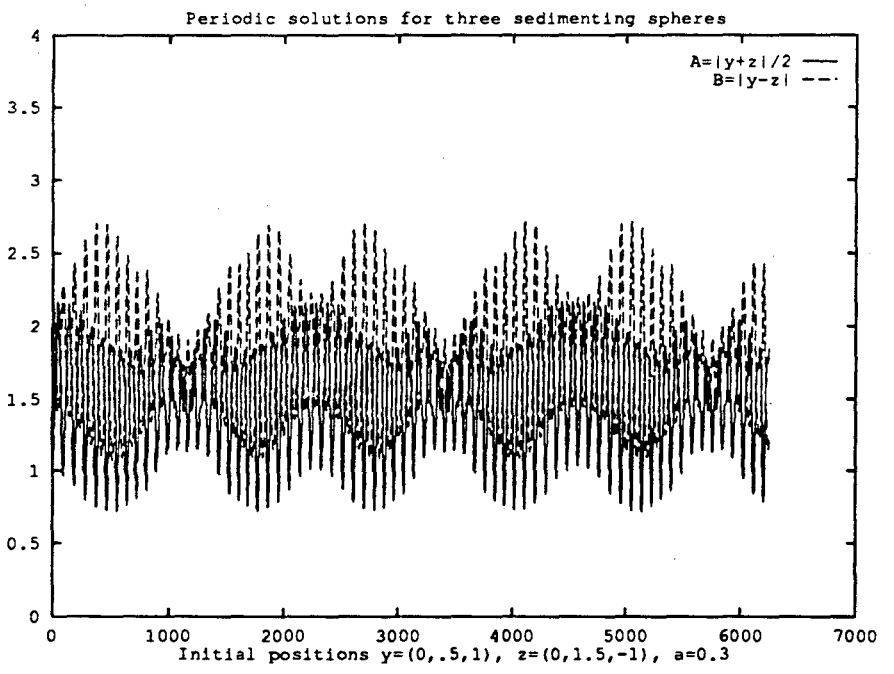

Figure 2.13: Asymmetric initial position, result 4

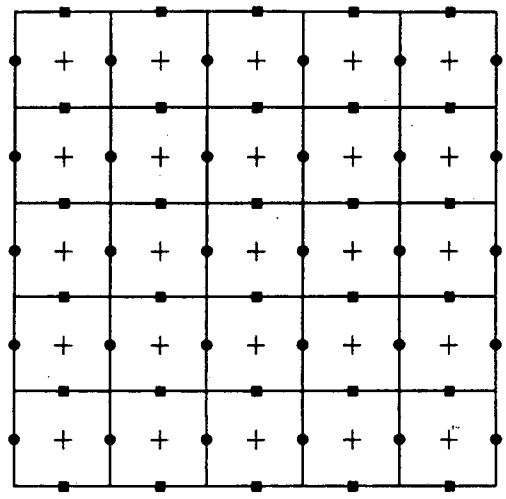

$\bullet \in U \quad \blacksquare \in V \quad + \in P$

Figure 3.1: Discretization of Domain

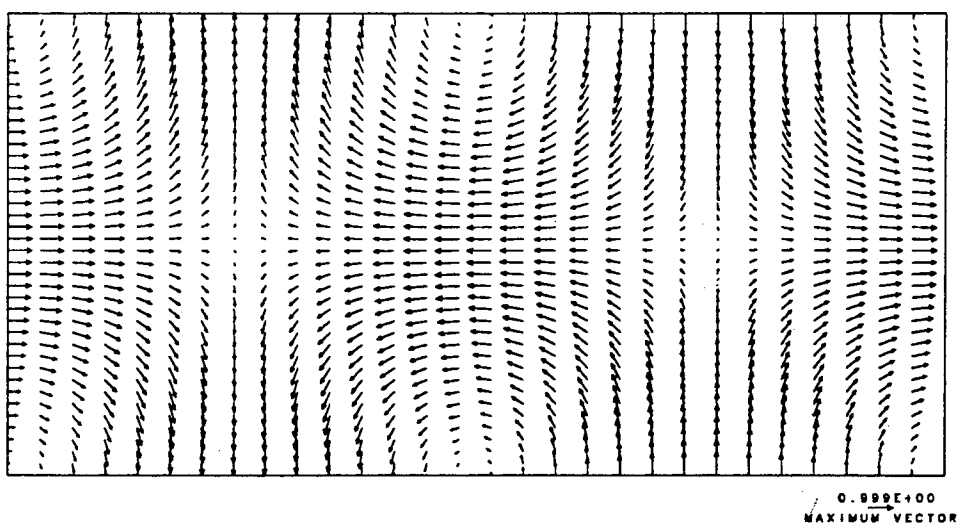

Figure 3.2: Velocity field of steady Stokes flow in 2-D

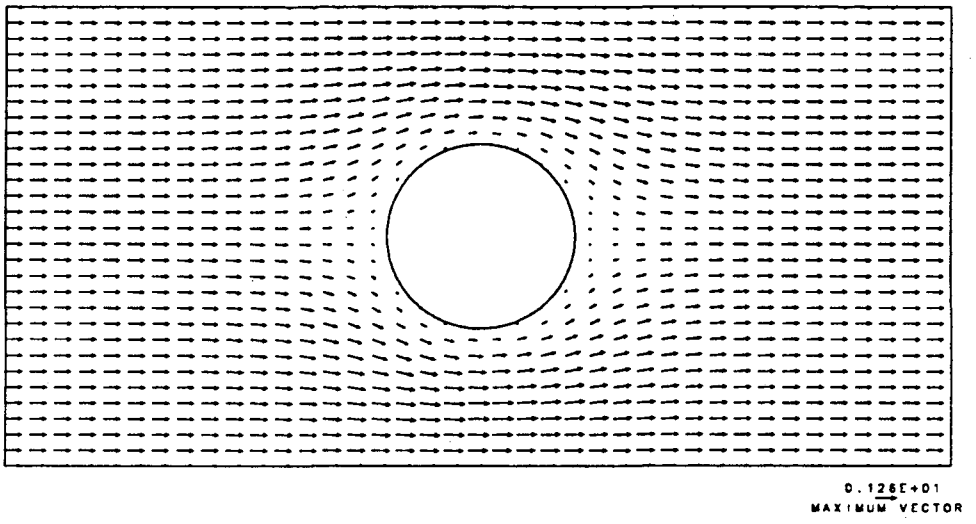

Figure 4.1: Velocity field of one sphere in a box

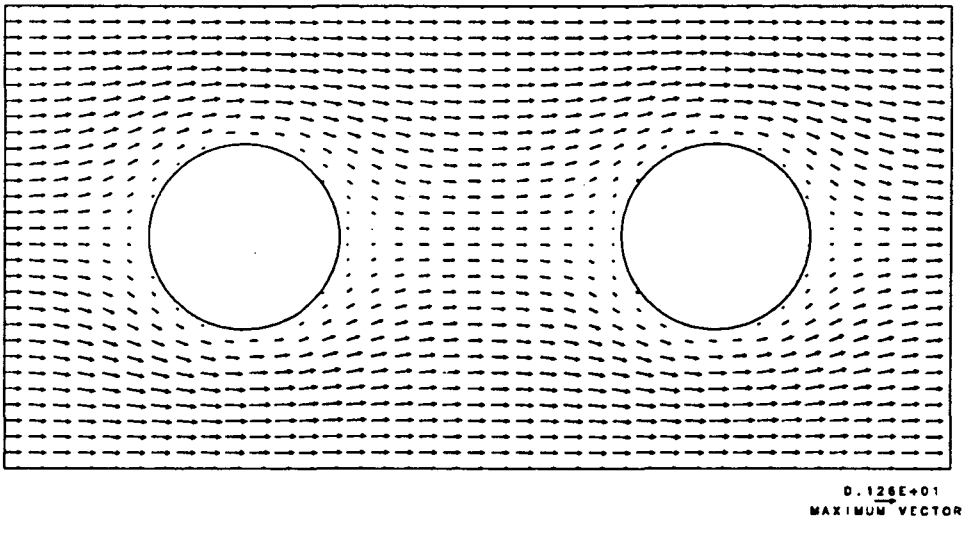

Figure 4.2: Velocity field of two spheres in a box

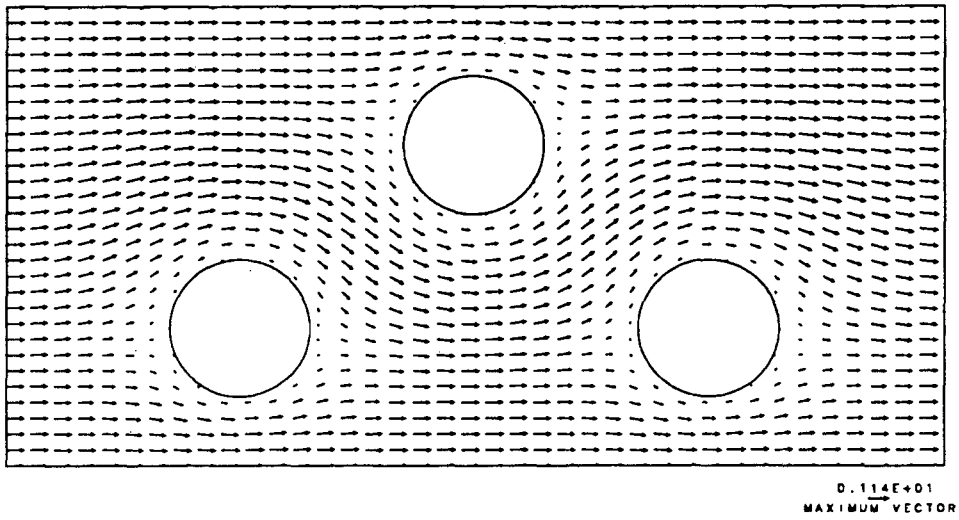

Figure 4.3: Velocity field of three spheres in a box

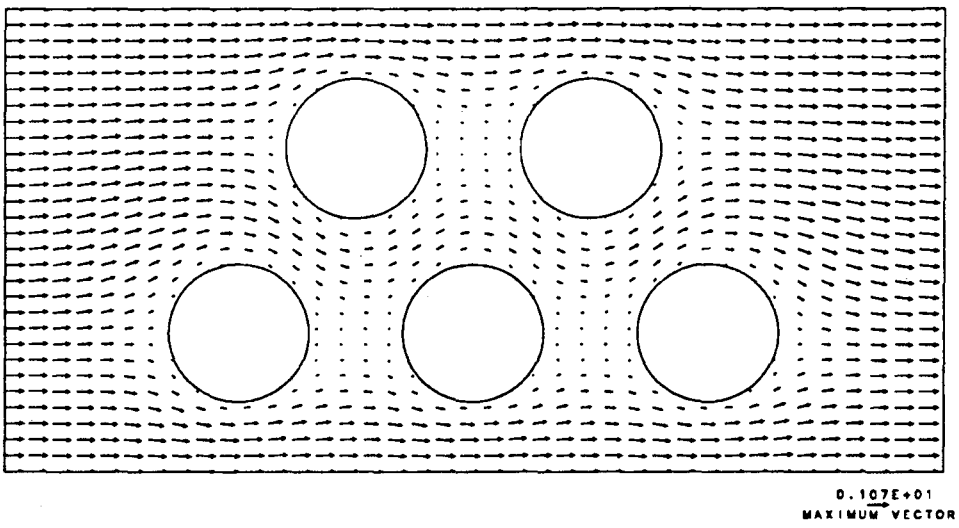

Figure 4.4: Velocity field of five spheres in a box

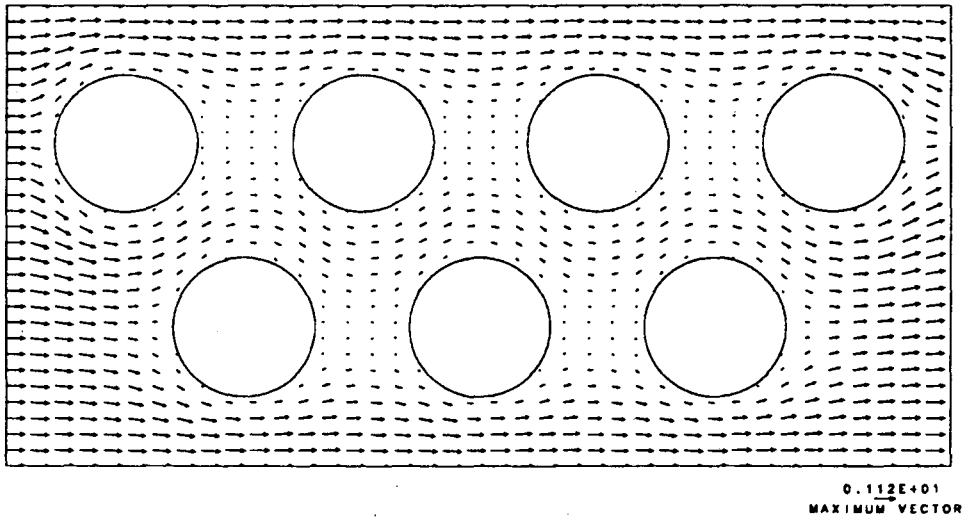

Figure 4.5: Velocity field of seven spheres in a box

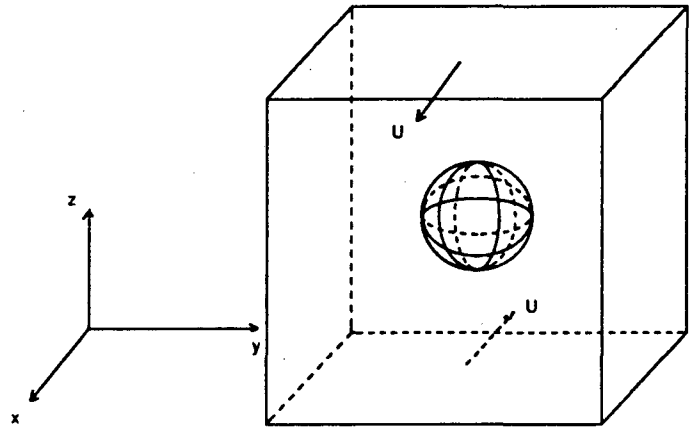

Figure 4.6: Shear flow suspension with one sphere

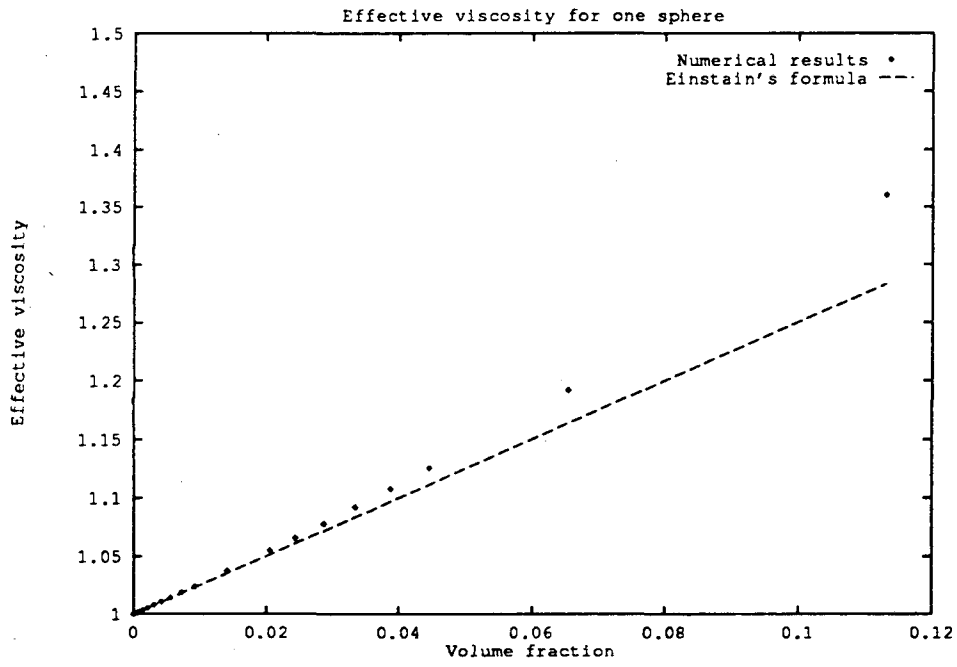

Figure 4.7: Effective viscosity of shear flow suspension with one sphere

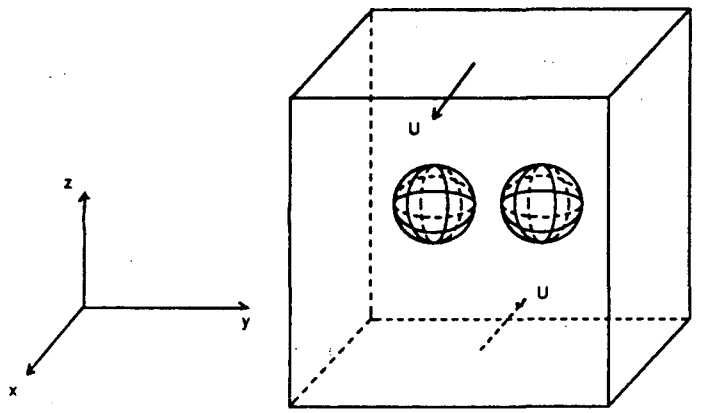

Figure 4.8: Shear flow suspension with two sphere

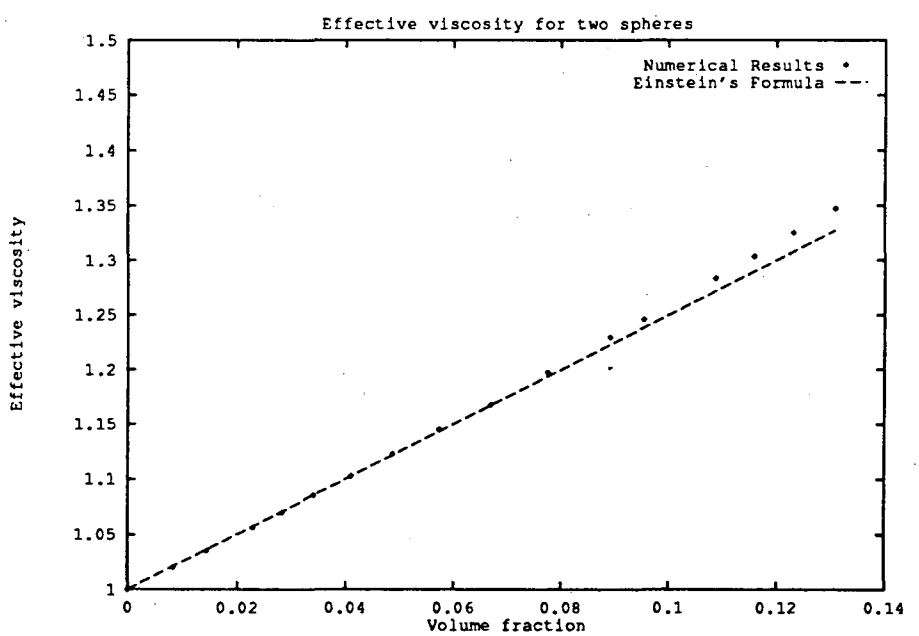

Figure 4.9: Effective viscosity of shear flow suspension with two spheres

LAWRENCE BERKELEY LABORATORY
UNIVERSITY OF CALIFORNIA
INFORMATION RESOURCES DEPARTMENT
BERKELEY, CALIFORNIA 94720